European Journal of Medicinal Chemistry 146 (2018) 687–708

Contents lists available at ScienceDirect

European Journal of Medicinal Chemistry

journal homepage: http://www.elsevier.com/locate/ejmech

Research paper

# Part III: Novel checkpoint kinase 2 (Chk2) inhibitors; design, synthesis and biological evaluation of pyrimidine-benzimidazole conjugates

Shadia A. Galal [a, *], Muhammad Khattab [a], Samia A. Shouman [b], Raghda Ramadan [c, d], Omaima M. Kandil [e], Omnia M. Kandil [f], Ashraf Tabll [g], Yasmine S. El Abd [g], Reem El-Shenawy [g], Yasmin M. Attia [b], Ahmed A. El-Rashedy [a], Hoda I. El Diwani [a]

[a] Department of Chemistry of Natural and Microbial Products, Division of Pharmaceutical and Drug Industries, National Research Centre, Cairo, 12622, Egypt
[b] Department of Cancer Biology, National Cancer Institute, Cairo University, Egypt
[c] Radiobiology Unit, Belgian Nuclear Research Center (SCK•CEN), Mol, Belgium
[d] Department of Basic Medical Sciences, Physiology Group, Ghent University, Ghent, Belgium
[e] Department of Animal Reproduction & Artificial Insemination, Division, of Veterinary Research, National Research Centre, Cairo, 12622, Egypt
[f] Department of Parasitology, Animal Disease, Division, of Veterinary, National Research Centre, Cairo, 12622, Egypt
[g] Department of Microbial Biotechnology, Division of Genetic Engineering & Biotechnology, National Research Centre, 12622, Cairo, Egypt

ARTICLE INFO

*Article history:*
Received 11 July 2017
Received in revised form
20 January 2018
Accepted 22 January 2018
Available online 2 February 2018

*Keywords:*
2-Phenylbenzimidazoles
Pyrimidines
Chk2 inhibitors
Cell cycle
Genotoxic anticancer therapies

ABSTRACT

Recently a dramatic development of the cancer drug discovery has been shown in the field of targeted cancer therapy. Checkpoint kinase 2 (Chk2) inhibitors offer a promising approach to enhance the effectiveness of cancer chemotherapy. Accordingly, in this study many pyrimidine-benzimidazole conjugates were designed and twelve feasible derivatives were selected to be synthesized to investigate their activity against Chk2 and subjected to study their antitumor activity alone and in combination with the genotoxic anticancer drugs cisplatin and doxorubicin on breast carcinoma, (ER+) cell line (MCF-7). The results indicated that the studied compounds inhibited Chk2 activity with high potency ($IC_{50} = 5.56$ nM - 46.20 nM). The studied candidates exhibited remarkable antitumor activity against MCF-7 ($IG_{50} = 6.6$ μM - 24.9 μM). Compounds **10a-c, 14** and **15** significantly potentiated the activity of the studied genotoxic drugs, whereas, compounds **9b** and **20**–**23** antagonized their activity. Moreover, the combination of compound **10b** with cisplatin revealed the best apoptotic effect as well as combination of compound **10b** with doxorubicin led to complete arrest of the cell cycle at S phase where more than 40% of cells are in the S phase with no cells at G2/M. Structure-activity relationship was discussed on the basis of molecular modeling study using Molecular modeling Environment program (MOE).



## 1. Introduction

Cancer is one of the main causes of death around the world that results from high rate of proliferation for abnormal cells [1,2]. Many factors, as infectious agents, tobacco, chronic inflammation and UV light, can lead to genomic instability which can stimulate cancerous injuries [1,2]. Radiotherapy and chemotherapy are often used in addition to surgery to decrease the probabilities cancer recurrence. The generic mode of chemotherapies, genomic instability results from targeting DNA in cancer treatment, the rapid emergence of drug resistance via development of chemo-resistance by cancer cells, have emphasized the urgent need to solve their shortcomings and find new strategy for cancer treatment [3,4]. The key components of the DNA damage response pathway are two kinases named as ataxia-telangiectasia mutated (ATM) and Rad3-related (ATR). They subsequently phosphorylate several substrates essential for DNA repair, cell cycle arrest, transcription, and apoptosis [5–9]. Cell cycle checkpoints represent the restriction points between each phase of the cell cycle whereby the entire process can be delayed/stopped its progress to enable the proper sequential of the process ensuring that each stage occurs in an imperative system or to allow time for DNA repair [10–12]. Downstream phosphorylation targets of ATM and ATR are the effectors serine/threonine checkpoint kinases 1 and 2 (Chk1& Chk2) [13], which in turn phosphorylate

* Corresponding author.
*E-mail addresses:* sh12galal@hotmail.com, sh12galal@yahoo.com (S.A. Galal).

https://doi.org/10.1016/j.ejmech.2018.01.072
0223-5234/

partially overlapping residues in other target proteins to induce cell cycle arrest and facilitate DNA repair. Chk1 is activated by ATR phosphorylation on Ser-317 and Ser-345 whereas Chk2 is activated by ATM phosphorylation on Thr-68 [14]. Downstream targets of Chk2 include Cdc25A and Cdc25C, which, on phosphorylation, go through degradation and cytoplasmic relocalization, respectively, and induce cell arrest at G1, S, and G2-M phases [15]. Another important target of Chk2 is p53, the phosphorylation of which on Ser20 regulates p53 transcriptional activation. Moreover, Chk2 phosphorylation of Hdmx Ser367, a negative regulator of p53, enhances its degradation [16,17] and endorses the accumulation of p53 and transcriptional induction of p53 responsive genes. Chk2 also phosphorylates the transcription factor E2F-1 on Ser364, thereby enhancing its stability and encourages apoptosis [18,19].

According to the current understanding of Chk2 function in tumor cells, in both biological and genetic context, Chk2 plays an important role in maintaining genomic integrity by acting as a signal transducer of DNA damage. Chk2 is endogenously activated in precancerous lesions with genomic instability and in cancer cells grown in culture. Studies have shown that the activated Chk2 acts as a survival factor for cancer cells. There are several rationales for the development of Chk2 inhibitors. First, wide range of anticancer drugs and ionizing radiation caused activation of Chk2 in tumor cells which seriously limited their effect in these cells [20–26]. These shortcomings of current chemotherapeutic approaches can be addressed by selective inhibition of Chk2. Second, inhibition of Chk2 in normal cells leads to protection normal tissues during chemotherapy or radiation therapy that increase the therapeutic indices of DNA-targeted and ionizing radiation(IR) agents in these cells. Therefore, Chk2 inhibitors would protect healthy tissues as well as sensitize the tumor to chemotherapy. Therefore, inhibition of Chk2 can address limitations of current cancer therapies and rationalize the basis of using Chk2 inhibitors as chemotherapeutic agents [27–30].

2-Arylbenzimidazole derivatives as 2-(4-(4-hydroxyphenylthio) phenyl)-*1H*-benzo[*d*]imidazole-5-carboxamide (1) (Fig. 1A) are defined as potent and selective inhibitors of Chk2 [31–33] and 4-fluoro-2-(4-{[(3S,4R)-4-(2-hydroxypropan-2-yl)pyrrolidin-3-yl] amino}-6,7-dimethoxyquinazolin-2-yl)phenol (XBJ) (Fig. 1B) were described as a new series of potent and selective ATP-competitive inhibitors of Chk2 that was generated on the basis of structure-based design [34]. A series of pyrazole-benzimidazole conjugates were developed by Galal et al. on the basis of structure based design such as *N*-isopropyl-2-(4-(3-methyl-4-nitro-1-phenyl-*1H*-pyrazol-5-yloxy)phenyl)-*1H*-benzo[*d*]imidazole-5-carboxamide (**2**) (Fig. 1C) [35] and 2-(4-(4-((2-carbamoylhydrazono)methyl)-3-methyl-1-phenyl-*1H*-pyrazol-5-yloxy)phenyl)-5-nitro-*1H*-benzo [*d*]imidazole (**3**) [36] exhibiting high potency as Chk2 inhibitors (Fig. 1D).

On the other hand, there are great numbers of antitumor active agents possessing the pyrimidine nucleus [37–41] such as pyrimidinylmethyl benzimidazole derivatives (**I**) (Fig. 2) which exhibited potent antitumor effect against panel of cancer cell lines [38] and AZD6738 (Fig. 1E) is orally active anti-tumor single agent acting as selective ATR inhibitor in phase I clinical trial and used in cancer treatment as a monotherapy or in combination with chemo/radiation therapy in patients with solid tumors [40,41].

The present study aimed to synthesize new candidates of 2-arylbenzimidazoles, on the basis of molecular hybridization of 2-arylbenzomidazoles and pyrimidines, guided by molecular docking studies, while assessing their biological activities not only as Chk2 inhibitors and antitumor agents, but also in combination with cisplatin or doxorubicin.

## 2. Results and discussion

### 2.1. Rational design

Although, 2-arylbenzimidazoles represent one of the most potent selective class of Chk2 inhibitors and showed effective radioprotection of human T-cells subjected to ionizing radiation during radiotherapy [31–33], their antitumor effect is not reported and so they cannot be used either as single agent in monotherapy treatment or in combined chemotherapies where they do not potentiate the antitumor effect of the genotoxic anticancer drugs [42]. To address their shortage and following the same strategy used in the formation of pyrazole-benzimidazole conjugates [35,36] which succeeded in the synthesis of new candidates of 2-arylbenzimidazoles with effective anticancer properties and potentiated antitumor effect of genotoxic drugs [35,36] that formed on the basis of hybridization two different bioactive molecules with complementary pharmacophoric functions or with different mechanisms of action often exhibited enhanced effects [43–45].

A small library 212 of pyrimidine-benzimidazole conjugates were designed by replacing the lateral aryl group of 2-arylbenzimidazoles **(II)** with pyrimidine moieties in formula I (Fig. 2). Most of the designed pyrimidine-benzimidazole conjugates of formula **III** (Fig. 2) revealed high binding affinities towards Chk2 receptor (PDB code: 2XBJ) [34] according to MOE program (supplementary material: Table 2S). Twelve synthetically feasible compounds were chosen among the best fifty candidates that exhibiting the highest binding affinities into Chk2 for chemical synthesis. Variation of the substituents permitted the deduction of structure-activity relationship. Finally, their possible interactions with Chk2 were investigated by docking using the MOE program into the crystal structure of Chk2 in complex with the potent and selective 2-(quinazolin-2-yl)phenol inhibitor (PDB code: 2XBJ) [34].

### 2.2. Chemistry

The target pyrimidine-benzimidazole conjugates were synthesized via straight forward synthetic routes as shown in Schemes 1–3. They were classified into three series according to the linker (X) between 2-phenylbenzimidazoles and pyrimidines moieties (Fig. 2). The desired pyrimidines derivatives **7a-g** have been achieved by synthesis of 6-aryl-4-oxo-2-thioxo-1,2,3,4-tetrahydropyrimidine-5-carbonitriles **(4a-f)** that were prepared following a previously described protocol [38,39]. The intermediate compounds, ethyl 2-(5-cyano-4-(4-florophenyl)-6-oxo-1,6-dihydropyrimidin-2-ylthio)acetate (**5**) and ethyl 2-(5-cyano-4-(4-chlorophenyl)-6-oxo-1,6-dihydropyrimidin-2-ylthio)acetate **(6)**, were obtained respectively by alkylation of compounds **4b** and **4c** with ethyl bromoacetate in benzene and potassium carbonate. Chloropyrimidine derivatives **7a-g** were obtained through treatment of hydroxypyrimidine derivatives **4a, 5, 4c, 4d, 4e, 4f** and **6**, respectively, with phosphorus oxychloride (Scheme 1).

The first series of target compounds **9a-c** and **10a-c** with ether linker (X = O, Fig. 2) was obtained by reaction of **7a-c** with 4-hydroxybenzaldehyde in DMF, potassium hydroxide and copper (I) iodide that yielded phenyl-pyrimidinyl ether derivatives **8a-c** in good yield. Subsequently, reaction of 3,4-diaminobenzoic with compounds **8a-c** in DMF and sodium thiosulphate afforded acid derivatives of 2-arylbenzimidazoles (**9a-c**). Finally, coupling of 2-arylbenzimidazoles **9a-c** with ammonium carbonate in DMF and CDI yielded amides of analogues of 2-arylbenzimidazoles **10a-c** (Scheme 2).

The second series of pyrimidine-benzimidazole conjugates

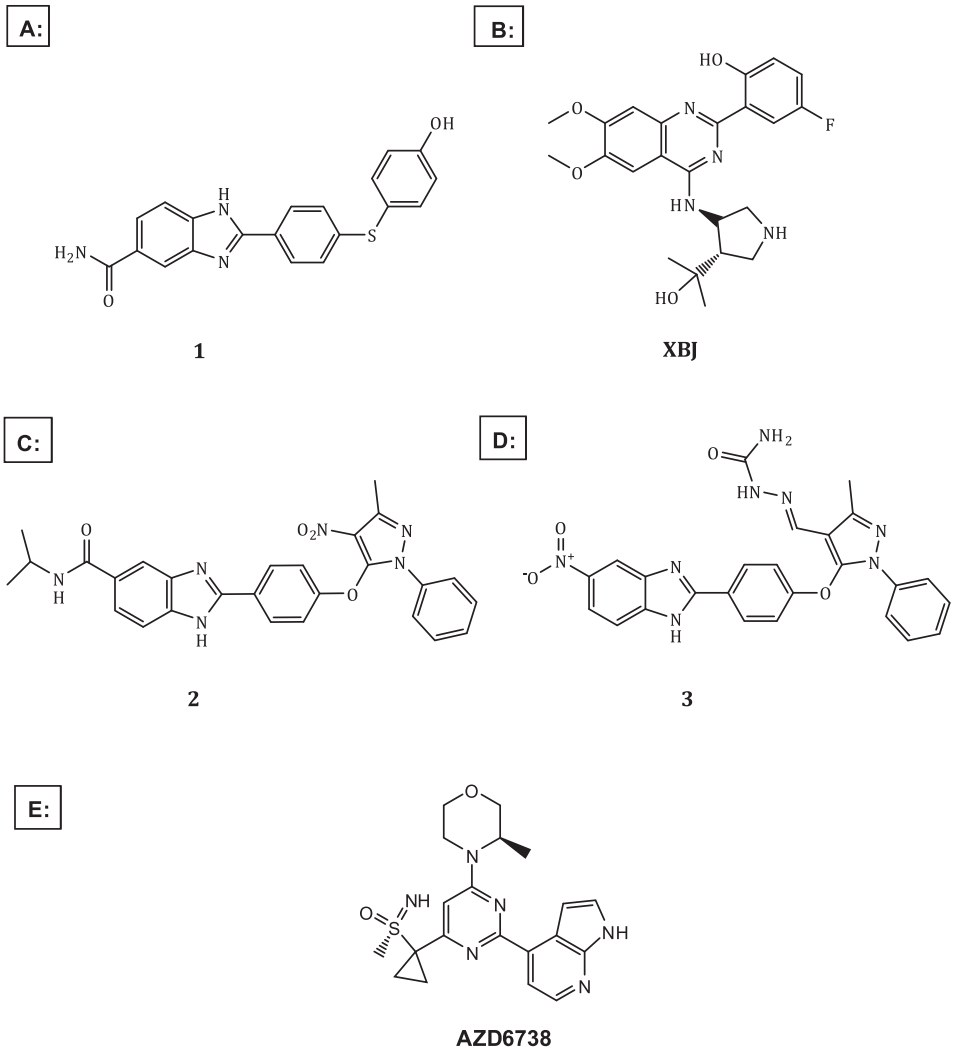


**Fig. 1. A-E:** Reported potent Chk2 inhibitors (A–D) and AZD6738, potent antitumor active agent with selective inhibition against ATR (E).

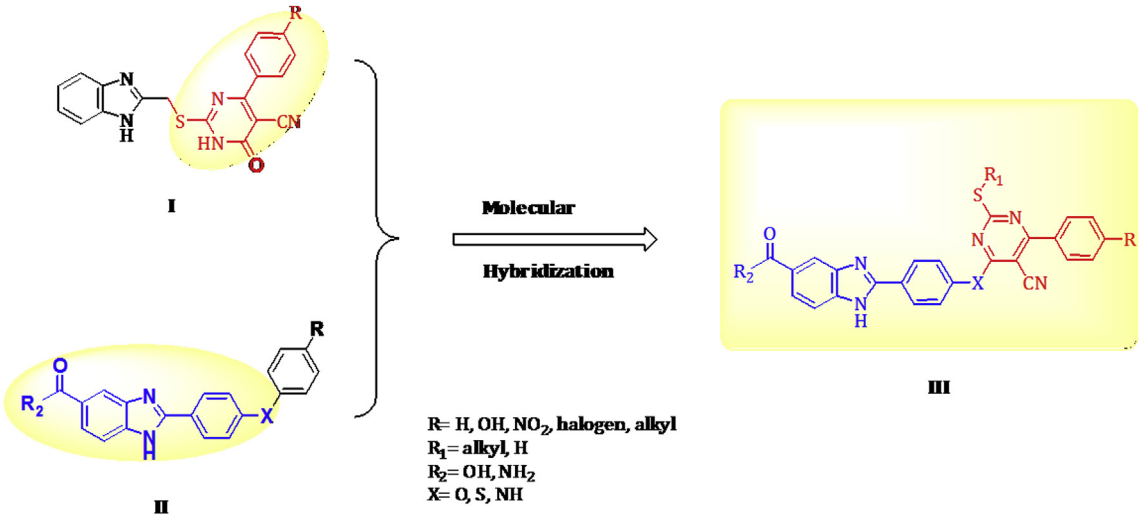


**Fig. 2.** Rational design of the target pyrimidine-benzimidazole conjugates via hybridization of effective antitumor active agents (I) and selective Chk2 inhibitors (II).

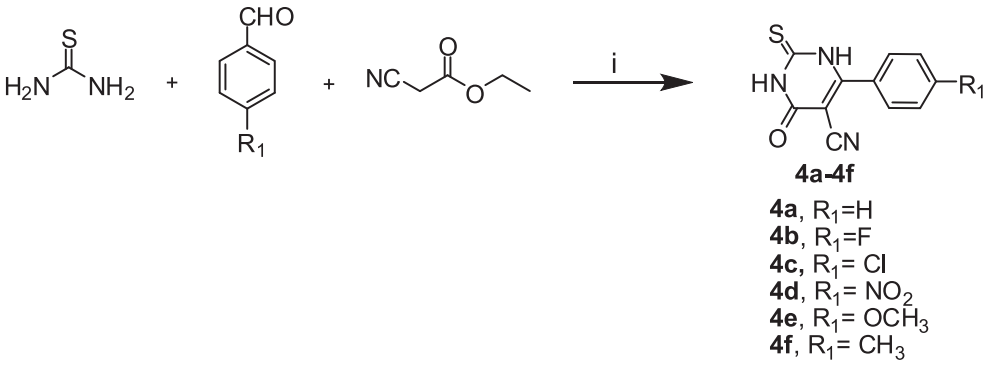


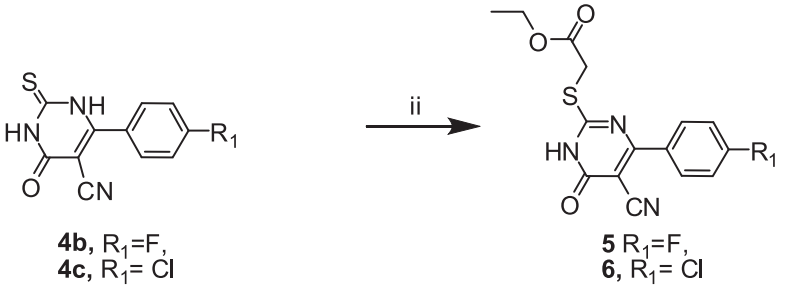


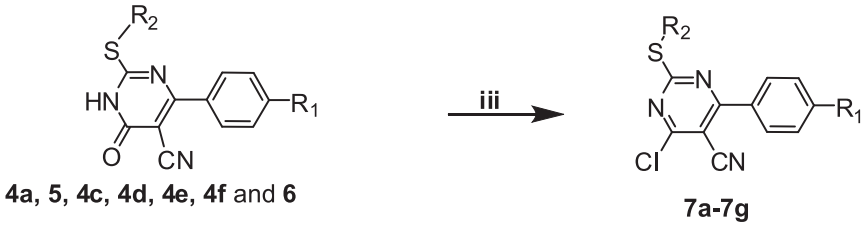


| Compound | R1 | $R_2$ |
|---|---|---|
| **7a** | H | H |
| **7b** | F | $CH_2COOC_2H_5$ |
| **7c** | Cl | H |
| **7d** | $NO_2$ | H |
| **7e** | $OCH_3$ | H |
| **7f** | $CH_3$ | H |
| **7g** | Cl | $CH_2COOC_2H_5$ |

**Conditions: i) $K_2CO_3$, ethanol, reflux, 6h, ii) ethyl bromoacetate, $K_2CO_3$, benzene, reflux, 3h, iii) $POCl_3$, stirring, 50 °C, 3h,**

**Scheme 1.** Synthetic routes of chloropyrimidine derivatives **7a-g.**

**12**–**15** (Scheme 3) with amino linker (X = NH; Fig. 2) were obtained by reaction of chloropyrimidines **7d,e** with 4-aminobenzoic acid to form pyrimidinyl aminobenzoic acid derivatives **11a,b** in the presence of DMF, potassium hydroxide and catalytic amount of copper (I) iodide. Then, 3,4-diaminobenzoic acid was reacted with compounds **11a,b** in polyphosphoric acid to form acid derivatives of 2-arylbenzimidazoles **12** and **13**, respectively. Finally, coupling of **12** and **13** with ammonium carbonate in the presence of CDI and DMF yielded the target amides of pyrimidine-benzimidazole conjugates **14** and **15,** respectively (Scheme 3).

The third series of pyrimidine-benzimidazole conjugates **16**–**23** with thio-ether linker (Scheme 3) obtained via similar steps that started by reaction of chloropyrimidines **7c, 7e, 7f** and **7g** with 4-mercaptobenzoic acid to form phenyl pyrimidine thio-ether derivatives **11e, 11c, 11d,** and **11f**, respectively, in the presence of potassium hydroxide, catalytic amount of copper (I) iodide and DMF. Thio-ether derivatives **11c-f** were reacted with 3,4-diaminobenzoic to afford pyrimidine-benzimidazole conjugates of thioether linker **16**–**19** which followed by formation of the target amides analogues **20**–**23** via coupling with ammonium carbonates (Scheme 3).

The synthesized compounds were characterized by physicochemical and spectral means. The MS, $^{1}$HNMR, $^{13}$CNMR spectral data and elemental analyses were found in accord with the assigned molecular structures.

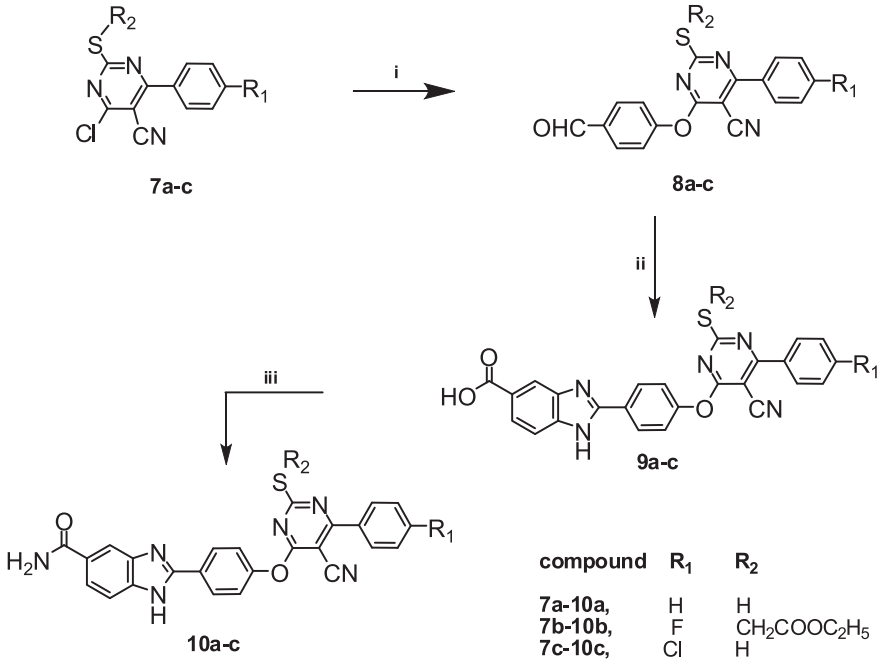


Conditions: i) 4-hydroxybenxalehyde, KOH, DMF, CuI, 70 °C, 2h, ii) 3,4-diaminobenzoic acid, $Na_2S_2O_5$, DMF, reflux, 24 h, iii) $(NH_4)_2CO_3$, CDI, DMF, stirring, r.t., 24 h.

**Scheme 2.** Synthetic routes of pyrimidine-benzimidazole conjugates **9a-c** and **10a-c.**

### *2.3. Evaluation of the efficacy of target compounds as Chk2 inhibitors*

The checkpoint Kinase Assay was used to demonstrate the chemical inhibition of Chk2 function by compounds **9a-c, 10a-c, 14, 15** and **20**–**23**. The $IC_{50}$ values of synthesized compounds as Chk2 inhibitors in addition to 2-(4-(4-hydroxyphenylthio)phenyl)-1*H*-benzo[*d*]imidazole-5-carboxamide (**1**) as lead compound have been evaluated (Table 1). The activity of synthesized compounds has not been examined against other kinases. The determination of $IC_{50}$ of studied compounds against Chk2 function profile, the newly synthesized 2-arylbenzimidazoles are effective potent inhibitors against Chk2 (Table 1) with $IC_{50}$ in a range from 5.56 nM to 46.20 nM. Six candidates (**9b, 23, 9a, 14, 9c** and **20**) out of twelve synthesized 2-phenylbenzimidazoles were found to be more potent than the lead compound **1** ($IC_{50} = 32.40$ nM). Compounds **9b** and **23** are the most potent derivatives ($IC_{50} \simeq 5.55$ nM). Compounds **10a, 10b, 21, 15** and **10c** exhibited comparable inhibitory effect with the lead compounds. In the first series with ether linker, acid conjugates **9a-c** are more potent than the amides analogues **10a-c**. In the second series with amino linker, compound **14** is more effective than compound **15**. In the third series with thioether linker, compound **22** ($IC_{50} = 46.20 \pm 3.44$ nM) showed the least potency among the studied compounds. The order of activity is as follows: **23** = **9b, 9a, 14, 9c, 20, 10a, 10b, 21, 15, 10c** and finally **22** (Table 1).

### *2.4. Cytotoxicity of the synthesized Chk2 inhibitors and their combinations with doxorubicin and cisplatin*

The cytotoxicity of the studied compounds **9b, 10a-c, 14, 15** and **20**–**23** in addition, to two reference compounds (as a positive control) cisplatin and doxorubicin were tested on human breast cancer cell line (MCF7) using sulphorhodamine-B (SRB) assay [46] (Table 2). Compounds **9b, 10a-c, 14, 15** and **20**–**23** showed potential cytotoxicity on MCF7. The compounds **14** ($GI_{50} = 6.6 \pm 0.047$ μM), **15** ($GI_{50} = 7.1 \pm 0.01$ μM) and **23** ($GI_{50} = 6.2 \pm 0.07$ μM) showed higher cytotoxic effect than doxorubicin ($GI_{50} = 8.4 \pm 0.04$) while, a comparable toxicity to cisplatin was observed ($GI_{50} = 6.8 \pm 0.04$). On the other hand, compounds **9b, 10a-c** and **20**–**22** exhibited less potential cytotoxity than the two reference drugs, doxorubicin and cisplatin with $GI_{50}$ in range from ($11.7 \pm 0.07$ μM to $24.9 \pm 0.1$ μM). Preliminary structure activity relationships can be evaluated from the obtained results as follow: compound **9b** ($GI_{50} = 24.9 \pm 0.10$) is less cytotoxic than its amide analogue **10b** ($GI_{50} = 14.6 \pm 0.06$). For compounds **10a** ($GI_{50} = 20.2 \pm 0.02$) and **10c** ($GI_{50} = 11.7 \pm 0.07$), the presence of Cl in **10a** negatively affected on the activity. For amides of series 2, compounds **14** and **15** exhibited the highest activity among the studied compounds. For compounds **20**–**23** of series 3, compound **23** ($GI_{50} = 6.24 \pm 0.07$) is the most active compounds with obvious higher activity than its analogue **22** ($GI_{50} = 14.6 \pm 0.03$) that revealed the importance of presence of ethyl acetate group on thiol of pyrimidine moiety. For analogues **20** ($GI_{50} = 11.8 \pm 0.05$), **21** ($GI_{50} = 15.0 \pm 0.03$) and **22** exhibited comparable cytotoxic effect against MCF-7. Studying of SAR indicated that acid conjugate **9b** is less effective than its amide analogue **10b.** Ethyl thioacetate group is highly effective on the activity as observed in compound **23**. Compounds with amino linker as in compounds **14** and **15** are more effective as cytotoxic agents than that with ether or thio-ether linkers.

Resistance of the tumor to the used chemotherapy is a common phenomenon that can result in rapid disease progression during or

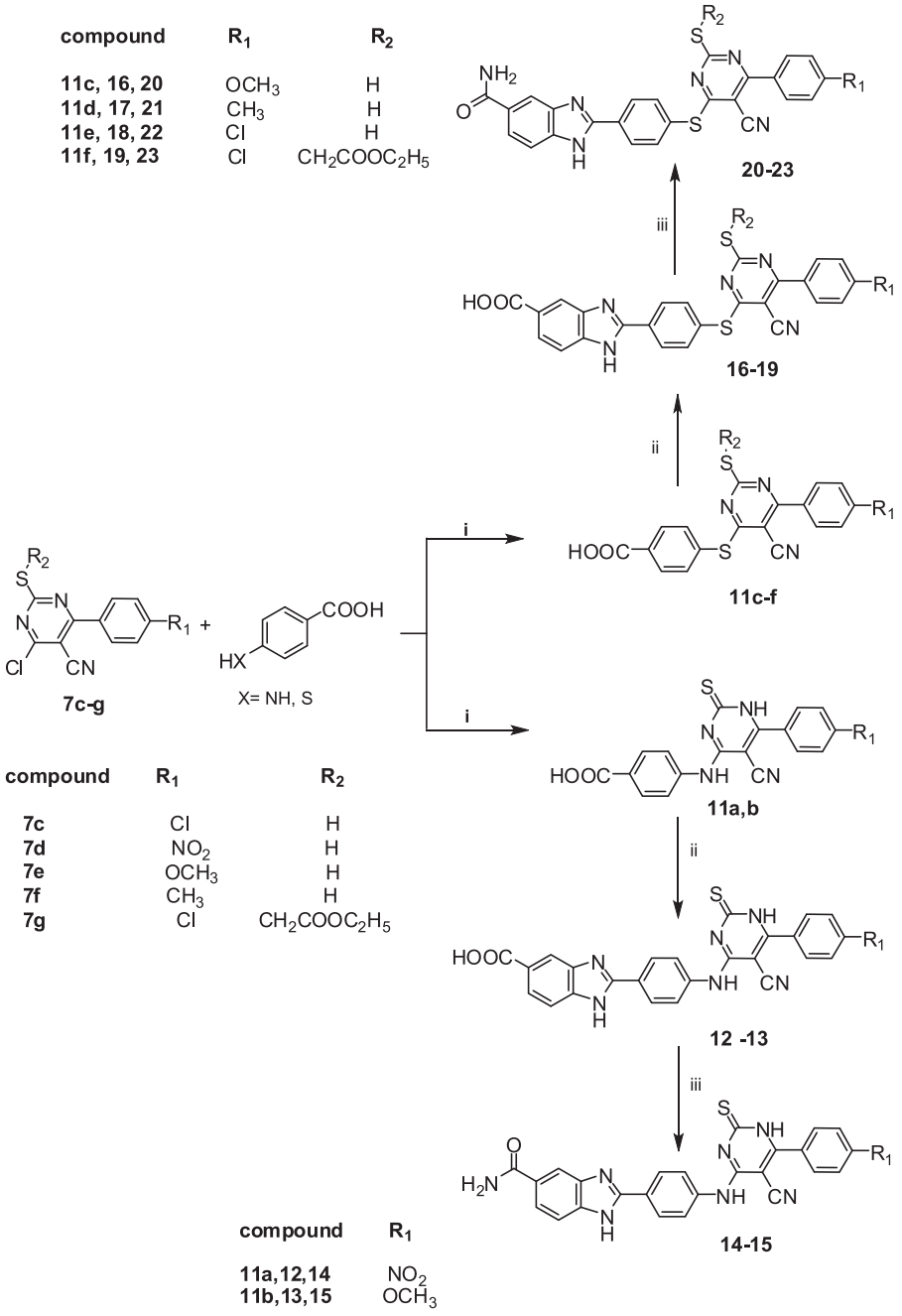


Conditions: i) KOH, DMF, CuI, 70 °C, 2h, ii) 3,4-diaminobenzoic acid, polyphosphoric acid, 150°C, 4h, iii) $(NH_4)_2CO_3$, CDI, DMF, stirring, r.t., 24 h.

**Scheme 3.** Synthetic routes of pyrimidine-benzimidazole conjugates **12**–**23.**

shortly after completion of treatment. One of the treatment modalities to overcome the impact of drug resistance is the concurrent use of two or more chemotherapy agents with different mechanisms of action and different modes of drug resistance. Therefore, one of the main goals of the present study was to investigate the combined effect of synthesized compounds **9b, 10a-c, 14, 15,** and **20**–**23** with genotoxic drugs as cisplatin and doxorubicin. In this study, combination effect was expressed as a potentiation index (PI), which is the ratio of $GI_{50}$ for the Chk2 inhibitor alone and $GI_{50}$ for the Chk2 inhibitor in combination with anticancer drug (Table 2). The studied compounds **10a-c,** and **14, 15** potentiated the cytotoxic effect of both doxorubicin and cisplatin (Table 2) with dramatic decrease in their $IG_{50}$. Compound **10b** exhibited the best potentiation effect with the highest PI whereas acid conjugate **9b** and compounds of series 3 with thio-ether linker **20**–**23** antagonize the cytotoxic effect of both drugs.

The foregoing results indicated that the synthesized compounds are effective as Chk2 inhibitors as well as effective antitumor

**Table 1**
Investigation of the activity of pyrimidine-benzimidazole conjugates **9a-9c**, **10a-10c**, **14**, **15** and **20**–**23** as Chk2 inhibitors.

| Compound# | $IC_{50}$ (nM) | Compound# | $IC_{50}$ (nM) |
|---|---|---|---|
| **9a** | 15.35 ± 4.36 | **14** | 25.80 ± 2.99 |
| **9b** | 5.56 ± 6.80 | **15** | 33.40 ± 3.27 |
| **9c** | 27.88 ± 6.66 | **20** | 28.00 ± 7.12 |
| **10a** | 31.00 ± 4.22 | **21** | 35.90 ± 9.41 |
| **10b** | 32.40 ± 2.07 | **22** | 46.20 ± 3.44 |
| **10c** | 33.80 ± 8.08 | **23** | 5.55 ± 4.09 |
| **1** | 32.40 ± 6.17 | | |

**1** = Lead compound; 2-(4-(4-hydroxyphenylthio)phenyl)-1*H*-benzo[*d*]imidazole-5-carboxamide.
$IC_{50}$: The concentration of synthesized compound that inhibits Chk2 by 50%.
$IC_{50}$ values expressed in nM ±SD, all values are the mean of at four replicate experiments.

**Table 2**
Cytotoxicity ($GI_{50}$) of studied compounds **9b**, **10a-c**, **14**, **15** and **20**–**23** alone and their combination with genotoxic drugs as Doxorubicin and Cisplatin against MCF7 cells.

| Compound | $GI_{50}$ (μM) | combination $GI_{50}$ (μM) | | PI | |
|---|---|---|---|---|---|
| | | Doxorubicin | Cisplatin | Doxorubicin | Cisplatin |
| **9b** | 24.90 ± 0.10 | >100 | >100 | <1 | <1 |
| **10a** | 20.25 ± 0.02 | 0.1 ± 0.02 | 0.06 ± 0.004 | 202.00 | 336.60 |
| **10b** | 14.60 ± 0.06 | 0.04 ± 0.02 | 0.04 ± 0.01 | 365.00 | 365.00 |
| **10c** | 11.70 ± 0.07 | 0.08 ± 0.08 | 0.1 ± 0.06 | 146.25 | 117.00 |
| **14** | 6.60 ± 0.04 | 0.05 ± 0.041 | ND | 132.00 | ND |
| **15** | 7.13 ± 0.01 | 0.09 ± 0.01 | 0.05 ± 0.05 | 78.80 | 142.00 |
| **20** | 11.80 ± 0.05 | >100 | >100 | <1 | <1 |
| **21** | 15.00 ± 0.03 | >100 | >100 | <1 | <1 |
| **22** | 14.61 ± 0.03 | >100 | >100 | <1 | <1 |
| **23** | 06.24 ± 0.07 | >100 | >100 | <1 | <1 |
| **DOX** | 8.40 ± 0.04 | | | | |
| **CIS** | 6.82 ± 0.04 | | | | |

Each value is the mean ± SD of 5 independent experiments performed in triplicates; the surviving fraction = O.D. (treated cells)/O.D. (control cells). [48].
$IG_{50}$: the concentration that inhibited growth by 50% relative to untreated cells.
PI: the ratio of the mean $GI_{50}$ for the ChK2 inhibitor alone and the mean $GI_{50}$ for the ChK2 inhibitor in combination with a cytotoxic agent.
The statistical significance of the results was analyzed using one-way ANOVA followed by Tukey multiple comparison test.

activity. The checkpoint kinase 2 (Chk2) is a critical enzyme involved in the DNA damage-response pathway, which is activated by phosphorylation prompting cellular response such as DNA repair, cell-cycle regulation or apoptosis. Moreover, inhibition of Chk2 is thought to sensitize p53-mutated or p53-deficient cancerous cells leading to cell death [47]. Due to their multiple pharmacological effects, the $IC_{50}$ (Table 1) that measure the degree of kinase inhibition of the synthesized compounds is different from $IG_{50}$ that is associated with cell death which may not confined by only one pathway (Table 2). Their activities as Chk2 inhibitors result from their binding to Chk2 receptor via interaction with its active sites as reported in the literature data bases of 2-arylbenzimidazoles class. So, we can deduce that there are different modes of actions controlling their inhibitory effect against Chk2 and their cytotoxicity on MCF-7 cells, which reflect the success of the hybridization of pyrimidine and 2-arylbenzimidazole in the production of molecules with complex modes of action that impact our multiple targets simultaneously that are better in controlling complex disease systems, less disposed to drug resistance and being the standard of care in cancer treatment [43,45].

### *2.5. Cellular inhibitory effect of synthesized compounds against Chk2 alone and in combination with genotoxic anticancer drug*

Several kinases in the DNA-repair pathway are activated after cells are exposed to cisplatin. Among the two kinases involved in checkpoint activation, namely ATM and ATR, cisplatin preferentially activates ATR kinase [47,48], which phosphorylates p53 at serine-15 to initiate activation of the p53 protein [49]. Also, cisplatin activates Chk2, but the effect of cisplatin on Chk2 appears to be independent of ATM [48,50,51].

The chemical evaluation of the synthesized compounds proved their potency as Chk2 inhibitors. It is important to determine their cellular inhibitory effects against Chk2 in cancer cells alone and in the combination with cisplatin. To address our target MCF-7 cells were exposed to single agent treatment with $IG_{50}$ of cisplatin, **9b**, **10b**, or their combination ($IG_{50}$ of cisplatin +0.1μ M of studied compound, **9b** or **10b**) (Fig. 3). Treated and untreated MCF-7 cells (negative control) were harvested, and proteins were extracted, separated on SDS-PAGE gel, transferred onto NC membrane and then probed with phosphorylated anti-Chk2 antibody [52,53]. The western blot reaction showed the immunogenic band recognized phosphorylation (activation) of Chk2 at 64.8 kDa which was observed in the untreated cancer cells (lane 4) and the cells treated with cisplatin alone (lane 3) and in combination of compound **9b** (lane 2) (Fig. 3). A complete disappearance of the immunogenic band of Chk2 phosphorylation reaction (activation process) in the cases of treating cells with $IG_{50}$ of compounds **9b** (lane 1), **10b** (lane 5) and the combination of **10b** with cisplatin (lane 6), was observed. These results suggest that the expression of Chk2 protein is induced by cisplatin [49,50] and its combination with **9b** whereas it was completely inhibited in combination of cisplatin and compound **10b** (Fig. 3). The specific blockade of Chk2 activity by compounds **9b** and **10b** as well as combination of **10b** with cisplatin in breast cancer cells proved that both compounds both **9b** and **10b** alone exhibited chemical inhibition of Chk2 activity but also the combined treatment of **10b** with cisplatin potentiates the kinase inhibitory effect of compound **10b** that suggest this combination may be important therapy for resistant types of tumors. Interestingly, combination of **9b** and cisplatin induced expression of Chk2 which indicated that the combined treatment of **9b** and cisplatin antagonized the inhibitory effect of **9b** which in accord with the observed antagonism effect for antitumor activity on MCF-7 cells in the potentiation assay.

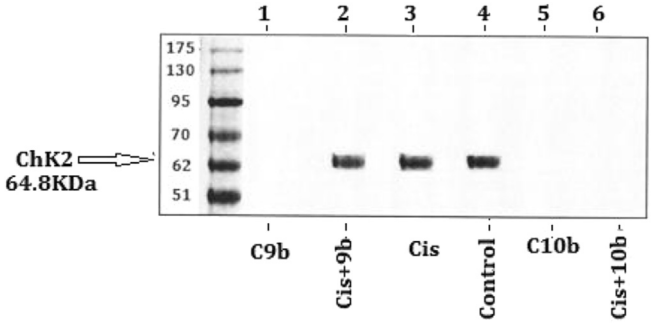


**Fig. 3.** Western Blot analysis showing reactivity of different samples on MCF-7 cells. Lane M: Pre-stained molecular weight marker, Lane 1: $IG_{50}$ of compound **9b** (**C9**) Lane 2: $IG_{50}$ of cisplatin +0.1μ M of compound **9b** (**Cis** + **C9b**), Lane 3: $IG_{50}$ of cisplatin (**Cis**), Lane 4: control, Lane 5: $IG_{50}$ of compound **10b** (**C10b**), Lane 6: $IG_{50}$ of cisplatin +0.1μ M of compound **10b** (**Cis** + **C10b**).

### 2.6. Effect of synthesized Chk2 inhibitors on apoptosis

The apoptotic effect was studied to further investigate anti-tumor activity of synthesized compounds. The experiments included untreated cells (control cells), treated MCF-7 cells with $GI_{50}$ of cisplatin, compound **9b** or **10b** alone or combination of $GI_{50}$ of cisplatin with 0.1 μM of synthesized conjugates **9b** or **10b** (Fig. 4A–G). As shown in Fig. 4F, combination of compound **10b** with cisplatin had the best apoptotic effect on the MCF-7 cells while cells treated with compound **9b** and cisplatin (Fig. 4D) showed the worst anti-apoptotic effect compared to the untreated cells (Fig. 4A). Regarding the MCF-7 cells treated with $IG_{50}$ of cisplatin, compounds **9b** and **10b**, the number of the living cells were 207 ± 8.54 (Fig. 4B), 284 ± 6.91 (Figs. 4C) and 232 ± 18.69 cells (Fig. 4E), respectively. These results can be summarized in Fig. 4G to reflect the antitumor activity of compounds **9b** and **10b** as well as

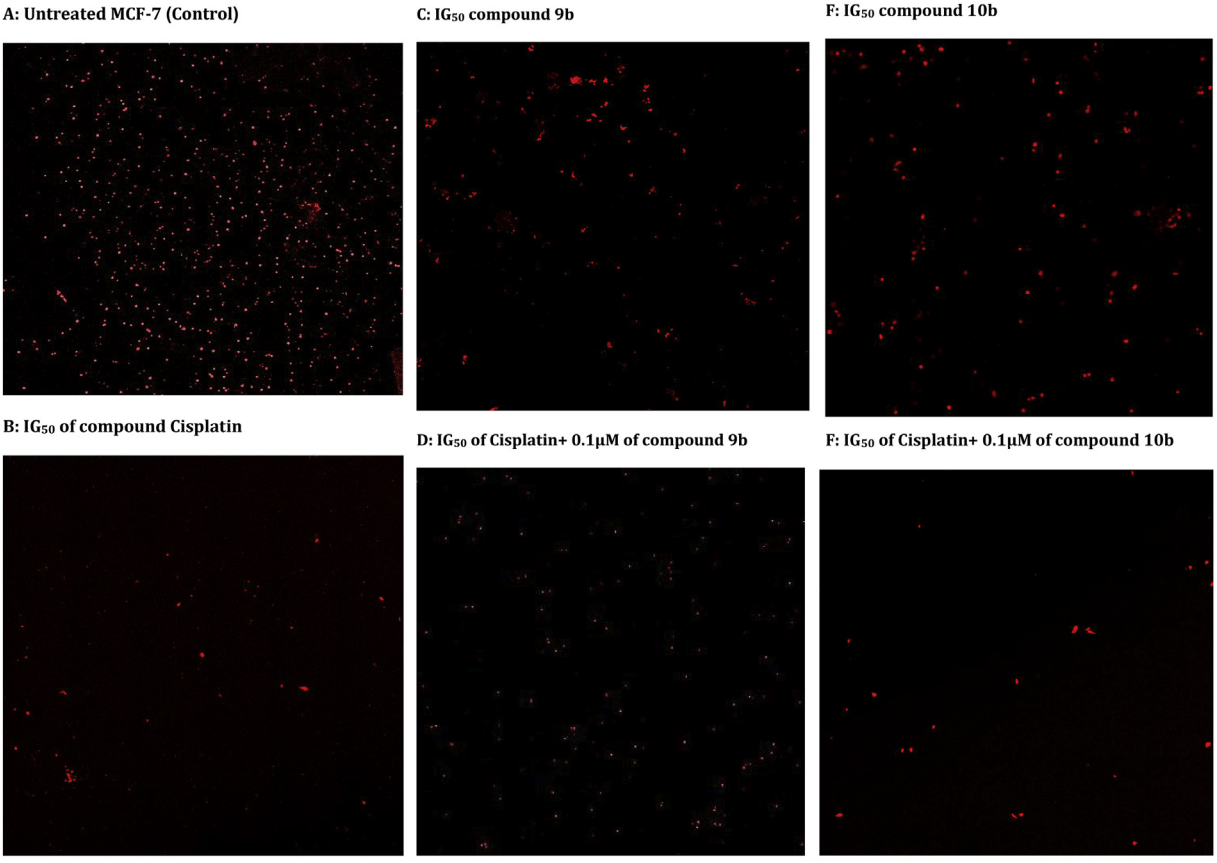


**G: Apoptotic effect of compounds 9b and 10b and their combination with cisplatin MCF-7**

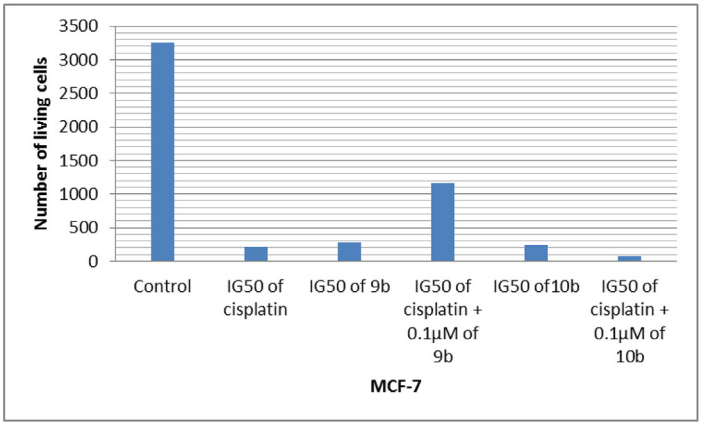


**Fig. 4. A-G:** Effect of synthesized Chk2 inhibitors on apoptosis of MCF7 cells. **A**, untreated cells (control). **B**, $GI_{50}$ of cisplatin alone. **C**, $GI_{50}$ of compound **9b**. **D**, $GI_{50}$ of cisplatin in combination with 0.1 μM of compound **9b**. **E**, $GI_{50}$ of compound **10b**. **F**, $GI_{50}$ of cisplatin in combination with 0.1 μM of compound **10b**. **G**, quantification of the apoptotic effect by calculating mean number of living cells in 5 point of dimension 1700 μm for each of stained with propidium iodide by using confocal microscope (Zeiss LSM 710), the objective lens is 20X and magnification 200X.

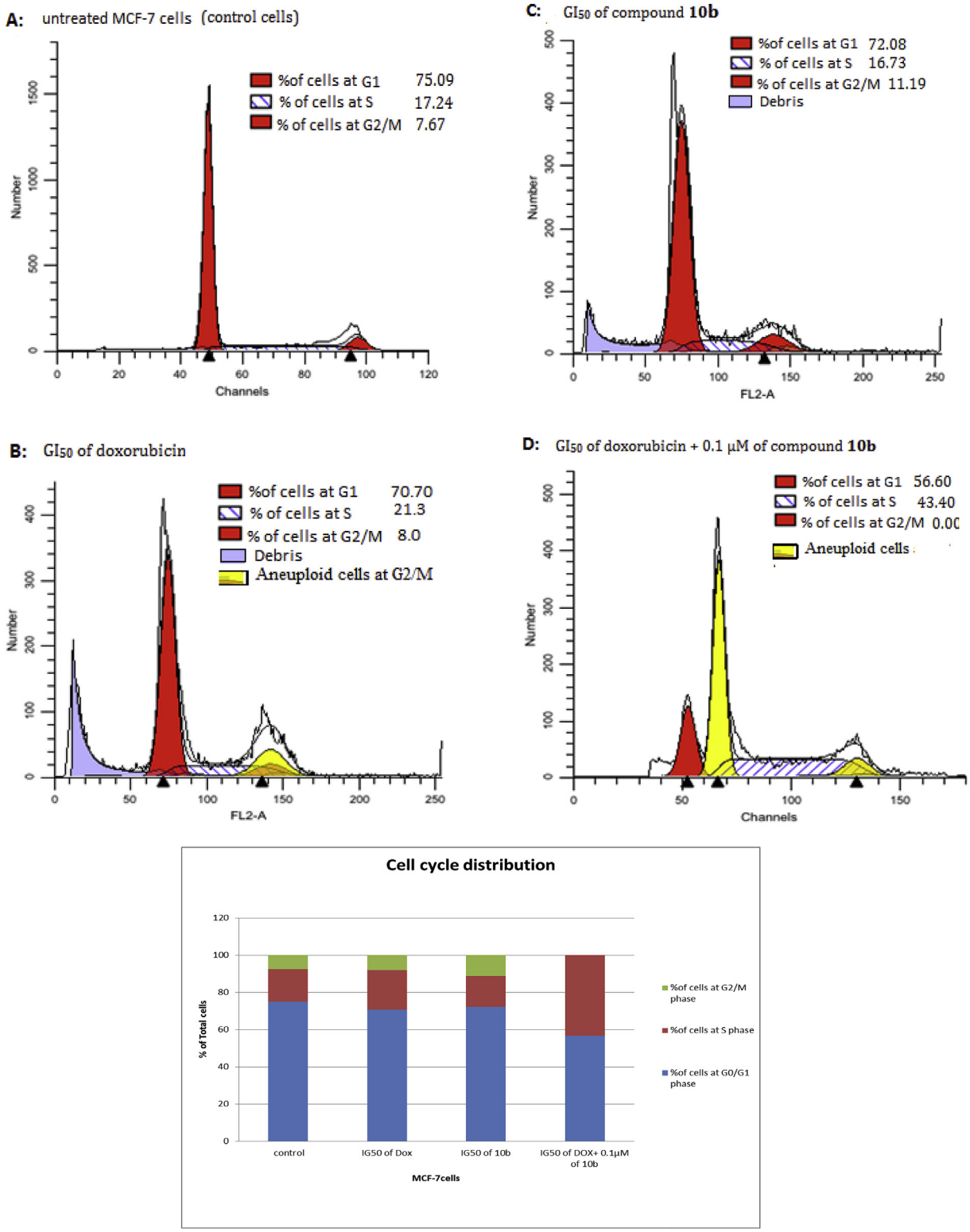


**Fig. 5. A-E**: Effects of compound **10b** on drug-induced cell cycle arrest in MCF-7 breast cancer cells. **A**, effects of cells treated with DMSO (control cells). **B**, effect of cells treated with $GI_{50}$ of doxorubicin alone. **C**, effects of cells treated with $GI_{50}$ of compound **10b**. **D**, effects of cells treated with $GI_{50}$ of doxorubicin in combination with 0.1 µM of compound **10b**. Histograms, cell cycle distribution were assessed by propidium iodide DNA staining as shown in Materials and Methods. **E**, quantification of the effects for total cells with studied concentrations of compound **10b** alone and in combination with doxorubicin-induced cell cycle arrest in MCF-7 cells at 48 h.

the potentiation effect of compound **10b** to the cytotoxicity of cisplatin in addition to the antagonism effect of compound **9b** to cisplatin.

### 2.7. Cell cycle analysis

Flow cytometry was used to check the activity of the synthesized Chk2 inhibitors on the cell cycle phases. The experiments were carried out on MCF-7 breast carcinoma cell line, including untreated cells (control cells), treated cells with $GI_{50}$ of compound **10b**, treated MCF7 cells with $GI_{50}$ of doxorubicin alone or $GI_{50}$ of doxorubicin in combination with 0.1 μM of compound **10b** (Fig. 5A–E). The analysis of control cells revealed that untreated cells showed the expected pattern for continuously growing cells and the existences of 75.09% of cells were in G1 phase, 17.24% in S-phase and 7.67% in G2/M phase (Fig. 5A). While treating cells with $GI_{50}$ of doxorubicin, the number of the arrested cells in S-phase increased (21.3%) and non-significant changes in the number of cells in phases of G1 and G2/M by comparison to control cells (Fig. 5B). Comparing the effect of compound **10b** with untreated control, compound **10b** alone arrested MCF7 cells at G2/M by 11.19% and almost no changes at G0/G1 phase (72.08%) or S phase(16.73%) of the cell cycle (Fig. 5C). These results suggest that the $G_2$-M phase accumulation was caused by an increase in the duration of the $G_2$-M phase. The combination of doxorubicin with compound **10b** caused obvious change on the cell cycle distribution by comparison to the effect of both doxorubicin or compound **10b** with significant arrest in S phase (43.8%) and a subsequent decrease in G1 to 56.6% and complete absence of cells in G2-M (Fig. 5D). This result suggests not only S phase accumulation but almost complete arrest of many cells in the S phase. A summary of the cell cycle distribution found in MCF-7 carcinoma cells treated with compounds **10b** and combination with doxorubicin with the studied concentrations compared to control cells at 48 h (Fig. 5E).

### 2.8. Molecular modeling

The molecular modeling of the target compounds **9a-c**, **10a-c, 14, 15** and **20–23** using MOE (molecular modeling environment) program was studied to get deeper insight into the molecular bases of the inhibitory potency and to find out the interaction between the new synthesized pyrimidine-benzimidazole conjugates and Chk2 receptor.

Molecular modeling calculations and local docking were done using MOE [54] to evaluate the binding free energies of these inhibitors into the target to Chk2 kinase receptor (PDB: (2XBJ).

#### 2.8.1. Validation of the docking performance and accuracy

To validate the docking accuracy of the program used, docking of the native co-crystallized XBJ (4-fluoro-2-(4-{[(3S,4R)-4-(2-hydroxypropan-2-yl)pyrrolidin-3-yl]amino}-6,7-dimethoxyquinazolin-2-yl)phenol) ligand of Chk2 kinase (PDB: (2XBJ) into the binding sites. The docked pose was docked superimposed on the native co-crystalized ligand on its binding sites with a root mean square deviation (RMSD) of 1.8 Å, S-score of −19.32 and bound by five hydrogen bonds (Fig. 6A–B).

#### 2.8.2. The binding affinities of the synthesized compounds into ChK2 receptor

All synthesized compounds were docked into same groove of the binding site of the native co-crystalized XBJ (4-fluoro-2-(4-{[(3S,4R)-4-(2-hydroxypropan-2-yl)pyrrolidin-3-yl]amino}-6,7-dimethoxyquinazolin-2-yl)phenol) ligand of Chk2 kinase into the binding sites and for docking calculations, the protein structure (PDB: (2XBJ) was first separated from the inhibitor molecule and refined using energy minimization with added hydrogens. Docking calculations were carried out using standard default variables for the MOE program [49].

The binding affinities were evaluated on the basis of the binding free energy S-score and hydrogen bonds with their distance between the designed compounds and the amino acids in the receptor (Table 3).

All the synthesized compounds **9a-c, 10a-c, 14, 15** and **20–23** gave higher score than the Lead compound; 2-(4-(4-hydroxyphenylthio)phenyl)-1*H*-benzo[*d*]imidazole-5-carboxamide **(1)** which docked into Chk2 with S-score fitness in a range from (−15.95 kcal/mol) to (−20.01 kcal/mol) (Table 3). Compounds **9b, 9a,** and **23** exhibited the highest score fitness of −20.01, −18.73 and −18.07, respectively (Table 3).

The active-site of amino acids residues in Lead compound formed one H-bond with GLU 308 and in the native ligand formed three hydrogen bonds with amino acids residue GLU 308, GLU 351 and MET 304 beside two H-bonds with $NO_3$ 1516. The synthesized compounds **9a-c, 10a-c, 14, 15** and **20–23** were bound into the binding site through up to two hydrogen bonds, to a higher extent with LYS 349, LYS 294, MET 304, $NO_3$ 1516 and GLY 232, and to a lower extent with ASN 269 (C=O), GLU 273, GLU 305 and ASP 368 amino acids (Table 3).

Compound **9b** showed the highest binding free energies (−20.0135 kcal/mol) among the studied compounds (Table 3). It also bound into ChK2 kinase by two hydrogen bonds into the binding site through its carboxylic group at position 5 with NH of Met 304 and its terminal cyano group with NH of LYS 249 (Fig. 7). The docking results for compound **9b** are highly correlated to its inhibitory activity against ChK2 kinase with highest activity among the synthesized compounds ($IC_{50} = 5.56 \pm 6.80$ nM).

Compound **10b** exhibited S-score fitness into Chk2 kinase receptor (−16.01 kcal/mol) comparable to lead compound **1** as well as they exhibited similar inhibitory activity against ChK2 ($IC_{50} = 32.40$) (Table 1). Compound **10b** also bound into the binding site of the receptor by two hydrogen bonds with MET 304 and LYS 349 (Fig. 8A–B) (Table 3). Compound **10b** and lead compound **1** revealed lower inhibitory activity than compound **9b** (Table 1).

Compound **9a** showed binding free energy (−18.73 kcal/mol) higher than lead compound (−15.56 kcal/mol). Also, **9a** showed better interaction than lead compound **1** by forming 2 H-bonds with the receptor binding site moieties MET 304 and LYS 249 and carboxylate at position 5 and terminal cyano of **9a**, respectively (Fig. 9) compared to only 1 H-bond between the lead compound and GLU308. The docking results for compound **9a** is correlated to its inhibitory activity against ChK2 kinase ($IC_{50} = 15.35 \pm 4.36$ nM) which is also higher than lead compound. The plausible binding modes and the docking orientations for compounds **9a**, **9b** and **10b** superimposed in the binding site of Chk2 receptor that are surrounded by a Gaussian contact surface are represented in Fig. 10.

#### 2.8.3. Structure-activity relationship

Structure-activity relationship was deduced from the forgoing results on the basis of molecular modeling by getting deeper insight into the molecular bases of the inhibitory potency (Table 1) and by correlating the interaction of pyrimidine-benzimidazole conjugates **9a-c, 10a-c, 14, 15, 20–23** and Chk2 receptor by the change in the binding free energy according to change of substituents (Table 3). Binding free energy score is a combination of different scoring functions includes H-bonds, ionic interaction, hydrophobic interaction, metal ligation and the interaction between hydrophobic and polar atoms. In the first series (X = O), the binding free energies of the acid derivatives, **9a-c**, are higher than the amide analogues **10a-c** (Table 3) which in accord with the observed higher inhibitory effect of the acid derivatives, **9a-c**, than the amide analogues **10a-c**

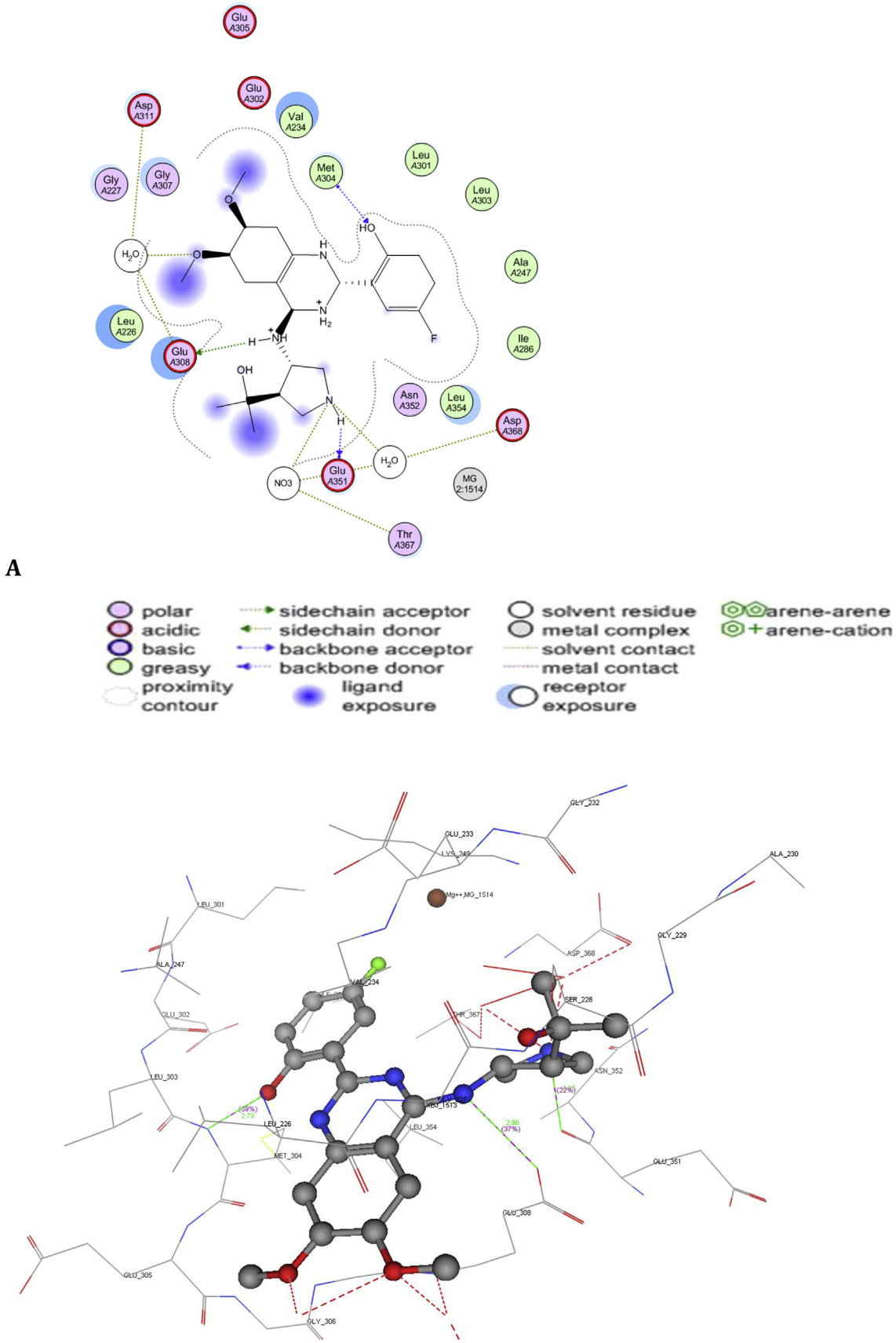


**Fig. 6. A-B**: Proposed binding mode for the interaction of the native co-crystallized ligand with Chk2 receptor (PDB: 2XBJ), five hydrogen bonds are formed with GLU 308, GLU 351, $NO_3$ 1516, MET 304, $NO_3$ 1516 (violet dotted lines), (A: 2D and B: 3D). (For interpretation of the references to color in this figure legend, the reader is referred to the Web version of this article.)

**Table 3**
Molecular Operating Environment (MOE) [54] flexible docking results for compounds **9a-c**, **10a-c**, **14**, **15** and **20**–**23** docked by (MOE) 2008.10 into Chk2 kinase (PDB: (2XBJ) in comparison to the co-crystallized XBJ ligand.

| Compound | S- score[a] (kcal/mol) | Hydrogen bonds between atoms of compounds and amino acids of receptor | | | | |
|---|---|---|---|---|---|---|
| | | Compounds | receptor | | Type | Distance (A˚) |
| | | Atoms | Atoms | Residues | | |
| **XBJ**[b] | −19.32 | H 4502 | OE 1322 | GLU 308 | H-don | 2.03 |
| | | H 4512 | O 2049 | GLU 351 | H-don | 2.23 |
| | | N 4511 | O2 4562 | $NO_3$ 1516 | H-don | 2.86 |
| | | O 4539 | N 1262 | MET 304 | H-acc | 2.79 |
| | | N 4511 | O2 4562 | $NO_3$ 1516 | H-acc | 2.86 |
| **1**[c] | −15.57 | H 4964 | OE 1322 | GLU 308 | H-don | 1.19 |
| **9a** | −18.73 | O 5152 | N 1262 | MET 304 | H-acc | 1.49 |
| | | N 5153 | NZ 2026 | LYS 349 | H-acc | 2.79 |
| **9b** | −20.01 | O 5152 | N 1262 | MET 304 | H-acc | 1.51 |
| | | N 5211 | NZ 2026 | LYS 249 | H-acc | 3.00 |
| **9c** | −16.43 | O 5152 | O1 4489 | $NO_3$ 1516 | H-acc | 1.92 |
| | | O 5152 | O1 4489 | $NO_3$ 1516 | H-don | 1.92 |
| **10a** | −16.95 | N 2403 | O2 2214 | $NO_3$ 1516 | H-acc | 2.55 |
| **10b** | −16.01 | H 5117 | O 1267 | MET 304 | H-don | 1.59 |
| | | O 5309 | NZ 2026 | LYS 349 | H-acc | 2.88 |
| **10c** | −16.22 | H 2418 | O1 2213 | NO3 1516 | H-don | 2.57 |
| **14** | −17.26 | N 2387 | N 150 | GLY 232 | H-acc | 2.85 |
| | | O 2415 | ND 338 | ASN 269 | H-acc | 3.13 |
| **15** | −16.42 | H 2422 | OE 365 | GLU 273 | H-don | 1.90 |
| | | N 2383 | N 150 | GLY 232 | H-acc | 2.52 |
| **20** | −17.50 | H 2422 | O 620 | GLU 305 | H-don | 1.55 |
| | | O 2409 | NZ 987 | LYS 349 | H-acc | 2.79 |
| **21** | −16.52 | O 2418 | N 1122 | ASP 368 | H-acc | 2.88 |
| **22** | −15.95 | N 2386 | N 150 | GLY 232 | H-acc | 2.99 |
| | | N 2403 | O2 2214 | $NO_3$ 1516 | H-acc | 2.60 |
| **23** | s | H 5013 | O 298 | ALA 230 | H-don | 2.25 |
| | | N 4998 | N 1262 | MET 304 | H-acc | 2.98 |

[a] Binding free energy.
[b] 4-Fluoro-2-(4-{[(3S,4S)-4-(1-hydroxy-1-methylethyl)pyrrolidin-3-yl]amino}-6,7-dimethoxy-quinazolin-2-yl) phenol.
[c] Lead compound: 2-(4-(4-hydroxyphenylthio)phenyl)-1*H*-benzo[*d*]imidazole-5-carboxamide (**1**).

(Table 1). For the acid candidates **9a-c**: compound **9b** is one of the most potent compound with the lowest $IC_{50} = 5.56$ nM and the highest binding free energy (S-score = −20.01 kcal/mol, Table 3). Decreasing of binding free energy by substitution with chlorine in **9c** (S-score = −16.43 kcal/mol) was observed and negatively affected the inhibitory effect ($IC_{50} = 27.88$ nM) compared to the unsubstituted **9a** (S-score = −18.73 kcal/mol, $IC_{50} = 15.35$ nM). For the amide analogues **10a-c**, comparable activities were detected ($IC_{50} \simeq 32$ nM) as well as comparable free energies (S-scores ≃ −16 kcal/mol) were found. For amides of the second series (compounds **14** and **15**, X = S), comparing the effect of the nitro group in compound **14** to that of the methoxy group in compound **15**, it can be deduced that the presence of the nitro group was more favorable for activity ($IC_{50} = 25.80$ nM) and led to enhancement of both, the binding free energy (S-score = −17.26 kcal/mol) and H-bonding interaction with the receptor, ($IC_{50} = 33.40$ nM, S-score = −16.42 kcal/mol). For the third series (**20**–**23**, X = NH), compound **23** exhibited the highest activity with a remarkable decrease in the $IC_{50}$ (5.55 nM) (Table 1) and an increase in the binding free energy (S-score = −18.07 kcal/mol, Table 3) with respect to its compound **22,** which exhibited the least potency among the studied compounds ($IC_{50} = 46.20$ nM, Table 1) and lowest S-score that reflecting the importance of ethyl thioacetate as substituent. This can be attributed to strong hydrophobic interaction with the receptor and H-bonding interaction with its carbonyl group which monopolizes the activity, no matters the compound was an acid with the ether linker as **9b** or an amide with amino linker as **23**, or the substituent on the phenyl ring was floro or chloro. For analogues **20, 21** and **22,** the $OCH_3$ substitution was favored as compound **20** was more active than **21** having $CH_3$ substitution, or Cl in **22,** which have negative effect on activity and causes a great decrease in the activity of **22,** which can be correlated with the increase of binding free energy in case of substitution with the methoxy group with respect to both methyl and chloro as substituents in compounds **21** and **22**, respectively.

## 3. Conclusion

The studied compounds **9b, 10a-c, 14, 15** and **20**–**23** exhibited potent inhibition effect against enzymatic activity of Chk2. The inhibitory effect of compounds **9b** and **10b** was also evaluated by western blot using anti-Chk2 which indicated that compounds **9b, 10b** and combination of **10b** with cisplatin blocked the enzymatic activity of Chk2 which was proved by complete disappearance of characteristic band of Chk2 at 64.8 KDa. Moreover, the studied compounds **9b, 10a-c, 14, 15** and **20**–**23** exhibited remarkable cytotoxicity against MCF-7. Compounds **10a-c, 14** and **15** potentiated the activity of both cisplatin and doxorubicin whereas compounds **9b** and **20**–**23** antagonized their cytotoxicity. The antitumor effect of compounds **9b** and **10b** was proved also by studying their apoptotic effect. Flow cytometry indicated that combination of compound **10b** with doxorubicin blocked the cell cycle to almost complete arrest in the S phase. The foregoing results necessitated further elucidation of pyrimidine-benzimidazole conjugates.

## 4. Material and methods

Microanalyses, spectral data of the compounds were performed in the Microanalytical National Research Centre and Pharmaceutical faculty, Cairo University, Egypt. The IR spectra (4000-400 $cm^{-1}$) were recorded using KBr pellets in a Jasco FT/IR 300E

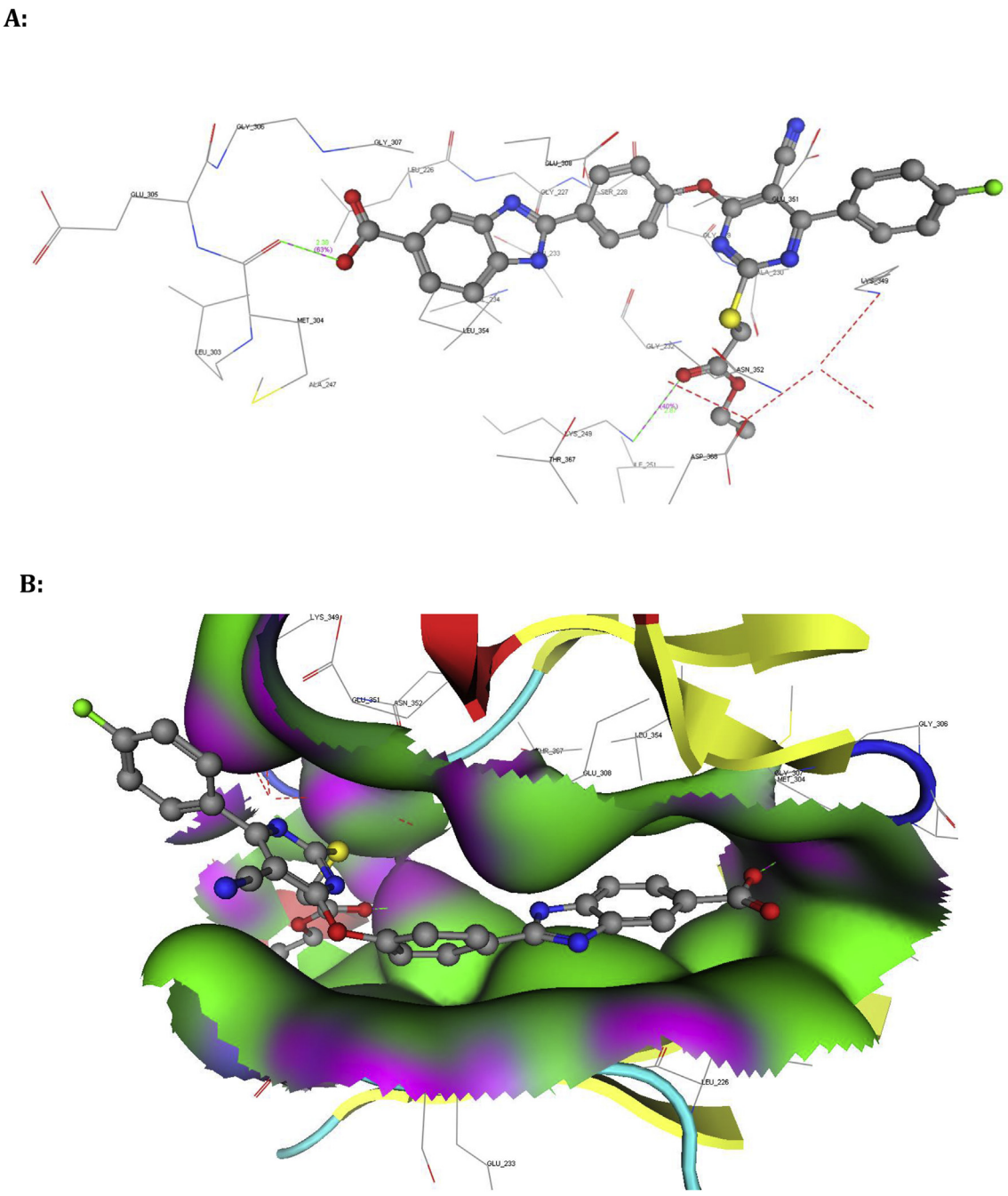


**Fig. 7. A-B:** Compound **9b** exhibited good fitting with ChK2 receptor (pdb: 2XBJ) via hydrogen bonds and hydrophobic interaction. Two direct H-bonds with Met 304 and LYS 249 are formed. Green line represents the distance of the hydrogen bonds and violet dots represent the score percentage of the H-bonds interaction with the receptor (**Fig. 7A**). Docking orientation of Compound 9b into ChK2 receptor (pdb: 2XBJ) receptor with a gaussian contact surface surrounding the van der Waals surface is drawn around the binding site (**Fig. 7B**). (For interpretation of the references to color in this figure legend, the reader is referred to the Web version of this article.)

Fourier transform infrared spectrophotometer on a Perkin Elmer FT-IR 1650 spectrophotometer. Starting materials, reagents, and solvents for reactions were reagent grade and used as purchased. Chromatography solvents were HPLC grade and were used without further purification. Thin layer chromatography (TLC) analysis was performed using Merck silica gel 60 F-254 thin layer plates. Flash column chromatography was carried out using columns prepacked with 40–63 μm silica or using standard chromatography techniques when performed on a large scale. NMR spectra were recorded on a Bruker Advance 300 MHz spectrometer. The samples were referenced to the appropriate internal non-deuterated solvent peak. The data is given as follows: chemical shift ($\delta$) in ppm, multiplicity (where applicable), coupling constants (J) in Hz (where applicable), and integration (where applicable). The mass spectra were recorded using a Finnigan mat SSQ 7000 (Thermo. Inst. Sys. Inc., USA) spectrometer at 70 eV. The used petroleum ether had a boiling temperature in the 60–80 °C range.

### 4.1. Molecular docking

The crystal structures of the Checkpoint kinase (PDB: 2XBJ) [34] in complex with its co-crystalized native ligand: (XBJ): (4-fluoro-2-

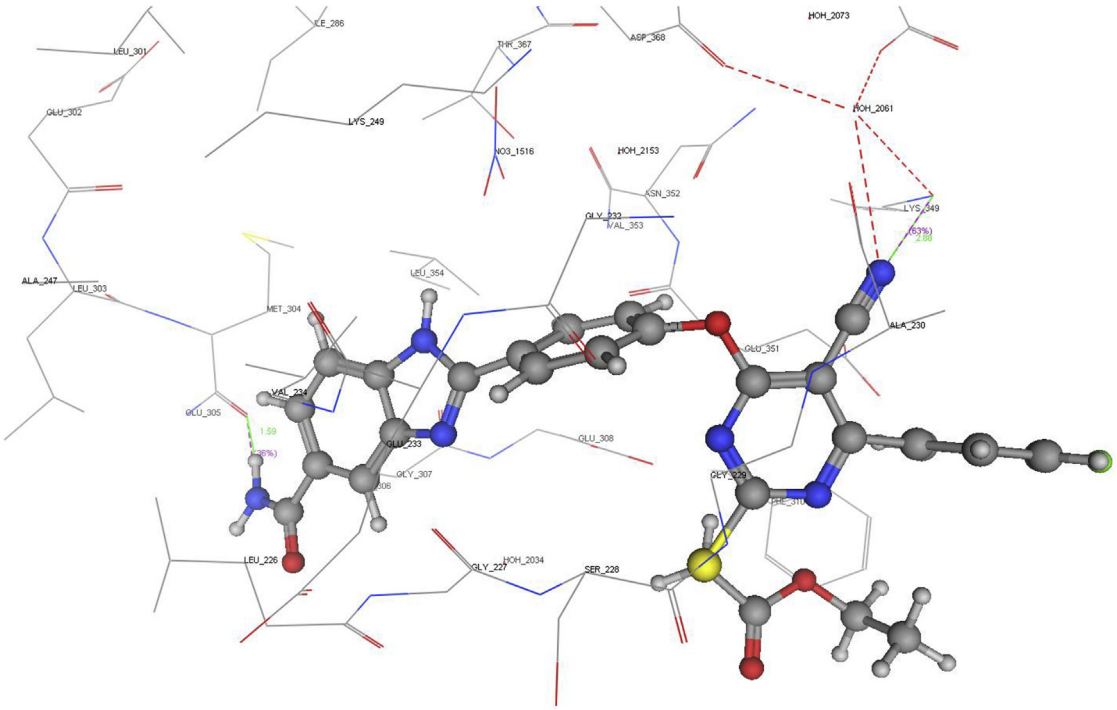


**B:**

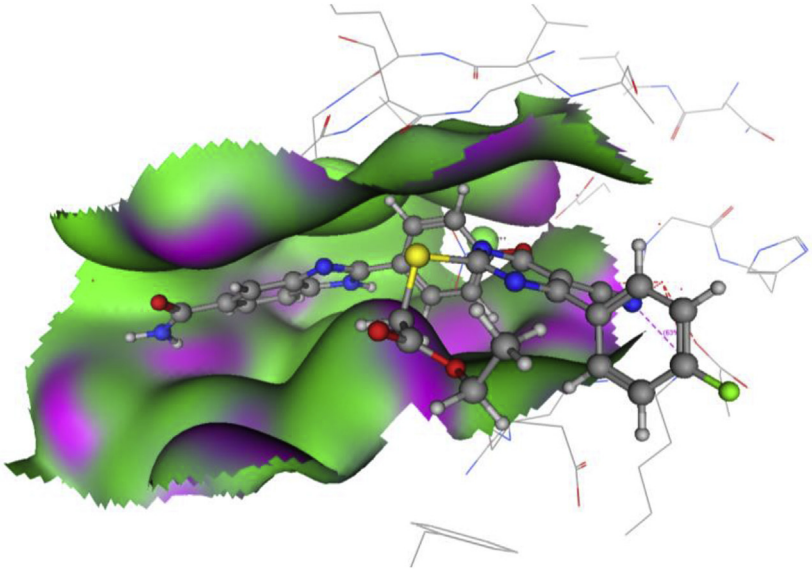

**Fig. 8. A-B:** The interaction of compound **10b** with Chk2 receptor (pdb: 2XBJ), 2 H-bonds are formed with MET 304 and LYS 349. Green line represents the distance of the hydrogen bonds and violet dots represent the score percentage of the H-bonds interaction with the receptor (**Fig. 8A**). Docking orientation of Compound 10b into ChK2 receptor (pdb: 2XBJ) receptor with a gaussian contact surface surrounding the van der Waals surface is drawn around the binding site (**Fig. 8B**). (For interpretation of the references to color in this figure legend, the reader is referred to the Web version of this article.)

(4-{[(3S,4R)-4-(2-hydroxypropan-2-yl)pyrrolidin-3-yl]amino}-6,7-dimethoxyquinazolin-2-yl)phenol), as a potent and selective Inhibitor of Checkpoint Kinase 2, was retrieved from the Protein Data Bank, http://www.rcsb.org/pdb/home/home.do. The key amino acids of the active site were identified using data in PDB sum, http://www.ebi.ac.uk/pdbsum.

- The constructed 3D structures of small library designed compounds about 200 derivatives were energetically minimized through Force field MMFF94x Optimization using gradient of 0.0001 kcal/mol.
- Validation of the MOE software by re-docking of the native co-crystalized on its binding site was done. The S-score is: −19.32 kcal/mol and RMSD is 1.8 Å

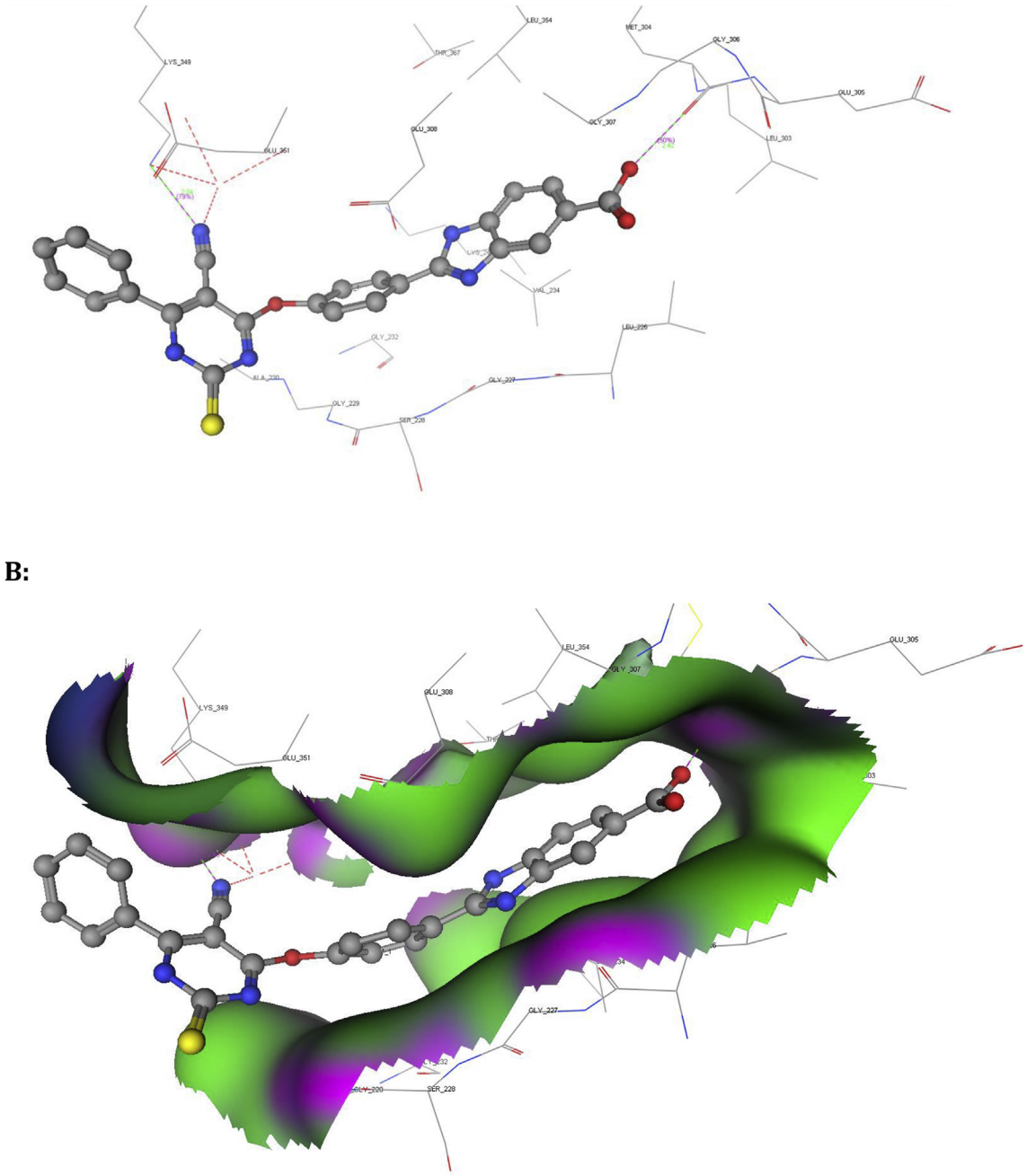


**Fig. 9. A-B**: The interaction of compound **9a** with Chk2 receptor (pdb: 2XBJ), 2 H-bonds are formed with MET 304 and LYS 349. Green line represents the distance of the hydrogen bonds and violet dots represent the score percentage of the H-bonds interaction with the receptor (Fig. 7A). Docking orientation of Compound **9a** into ChK2 receptor (pdb: 2XBJ) receptor with a gaussian contact surface surrounding the van der Waals surface is drawn around the binding site (Fig. 7B). (For interpretation of the references to color in this figure legend, the reader is referred to the Web version of this article.)

- Docking calculations were carried out using standard default variables for the MOE program and the tested compounds were docked in the binding site of the native co-crystalized ligand.
- The Dock scoring in MOE software was done using London dG scoring function, rotatable bonds were allowed; the best 10 poses were retained and analysed.
- The binding site of the human crystal structure of Chk2 is composed of the following amino acids: Leu226, Gly227, Val234, Ala247, Ile286, Leu301, Glu302, Leu303, Met304, Glu305, Gly307, Glu308, Glu351, Asn352, and Leu354.
- The binding free energy was used to rank the binding affinity of the synthesize compounds to Chk2 receptor. In addition, in case of compounds having simalr S-scores, hydrogen bonds between the ligand and amino acids in Chk2 receptors were used in the ranking of the compounds. Evaluation of the hydrogen bonds was done by measuring the hydrogen bond length which doesn't exceed 3 Å.
- Twelve compounds out of the best fifty were selected for chemical synthesis in this study and biological evaluations were performed as shown in the forgoing results.
- The mode of interaction of the native ligand 2XBJ receptors within their crystal structures was used as a standard docked model as well as for RMSD calculation.

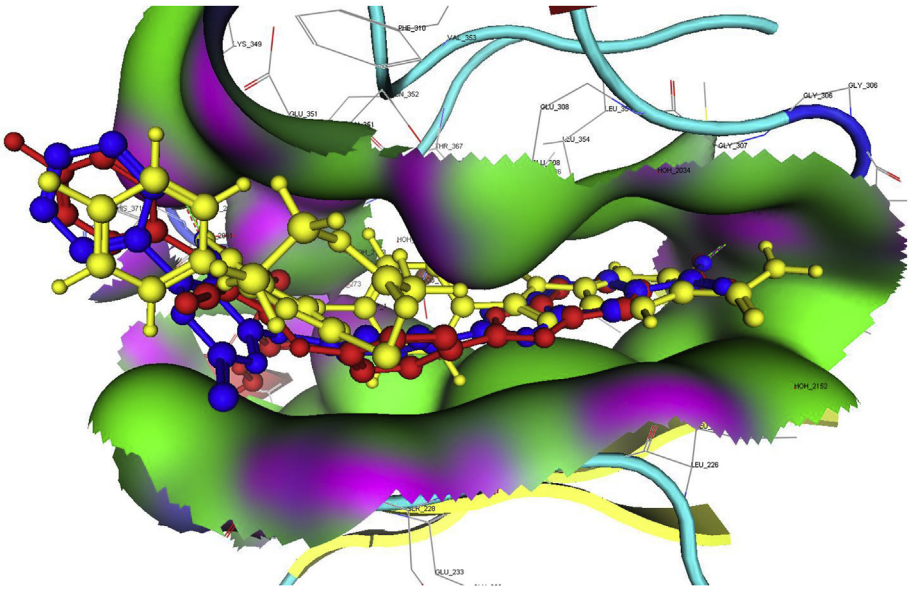

**Fig. 10.** Docking orientations and superimposition for Compound **9a** "colored in blue", compound **9b** "colored in red" along with ompound **10b** "colored in yellow" into ChK2 receptor (pdb: 2XBJ) receptor. A gaussian contact surface surrounding the van der Waals surface is drown around the binding site. (For interpretation of the references to color in this figure legend, the reader is referred to the Web version of this article.)

### 4.2. Chemistry

#### 4.2.1. Synthesis of compounds ***5*** and ***6***

A solution of 6-(4-fluorophenyl)-4-oxo-2-thioxo-1,2,3,4-tetrahydropyrimidine-5-carbonitrile **(4b)** or 6-(4-chlorophenyl)-4-oxo-2-thioxo-1,2,3,4-tetrahydropyrimidine-5-carbonitrile **(4c)** [39] (10 mmol) in benzene (50 mL) and $K_2CO_3$ (1.38g, 10 mmol) was treated with ethyl bromoacetate (1.66g, 10 mmol) added dropwise. The reaction mixtures were stirred for 1 h at room temperature then were refluxed for 3 h. The solvent was evaporated under reduced pressure. The solids obtained were filtered off and were crystalized from benzene as yellow crystals.

*4.2.1.1. Ethyl 2-(5-cyano-4-(4-florophenyl)-6-oxo-1,6-dihydropyrimidin-2-ylthio)acetate **(5)***. Yield, (84%), m.p. 159–162 °C. $^1$H NMR (300 MHz, DMSO) $\delta$ 1.03–1.12 (t, 3H, $CH_3$), 3.99–4.19 (m, 4H, $2CH_2$), 7.39–7.49(m, 2H), 7.96–8.07(m, 2H, 2H-Ar). $^{13}$C NMR (75 MHz, DMSO) $\delta$ 13.81, 32.93, 61.25, 93.00, 115.45, 115.57, 115.74, 115.81, 131.28, 131.34, 131.39, 130.77, 162.41, 165.12, 165.96, 165.74, 167.91. MS, *m/z* (%): 333(M+, 28%), Anal. Calcd for $C_{15}H_{12}FN_3O_2S$ (FW: 333): C, 54.05; H, 3.63; F, 5.70; N, 12.61; S, 9.62 Found: C, 54.21; H, 3.44; N, 12.54; S, 9.77.

*4.2.1.2. Ethyl 2-(4-(4-chlorophenyl)-5-cyano-6-oxo-1,6-dihydropyrimidin-2-ylthio)acetate **(6)***. Yield, (78%), m.p. 178–180 °C. $^1$H NMR (300 MHz, DMSO) $\delta$ 1.05–1.13 (t, 3H, $CH_3$), 4.09–4.20 (m, 4H, $2CH_2$), 7.34–7.37 (d, $J$ = 8.22 Hz 2H), 7.48–7.51 (d, $J$ = 8.22 Hz, 2H). MS, *m/z* (%): 351 (15%), 349 (44%) for $M^+$. Anal. Calcd for $C_{15}H_{12}ClN_3O_3S$ (FW: 349): C, 51.51; H, 3.46; Cl, 10.14; N, 12.01; S, 9.17. Found: C, 51.74; H, 3.55; Cl, 10.02; N, 12.22; S, 9.40.

#### 4.2.2. Synthesis of compounds ***7a-g***

Phosphorus oxychloride (20 mL) was added dropwise to compounds **4a**, **5, 4c, 4d, 4e, 4f** or **6** (10 mmol) with stirring at r.t for 1 h and then, stirred for 3 h at 50 °C. The reaction mixtures were left to cool to room temperature and then were added to ice bath with stirring. The yellow solids obtained were filtered off, washed with petroleum ether and crystalized from dichloromethane as yellow crystals of compounds **7a**, 7b, **7c-7f** [38] and **7g.**

*4.2.2.1. Ethyl 2-(4-chloro-5-cyano-6-(4-fluorophenyl)pyrimidin-2-ylthio)acetate **(7b)***. Yield (50%), m.p. 143–145 °C. $^1$H NMR (300 MHz, DMSO) $\delta$ 1.10–1.24 (t, 3H, $CH_3$), 4.07–4.20 (m, 4H, $2CH_2$), 7.37–7.40(m, 2H), 8.10–8.13(m, 2H, 2H-Ar). MS, *m/z* (%):351 (58%), 353 (19%) $M^+$. Anal. Calcd for $C_{15}H_{11}ClFN_3O_2S$ (FW: 351): C, 51.21; H, 3.15; Cl, 10.08; F, 5.40; N, 11.94; S, 9.11. Found: C, 51.09; H, 3.17; Cl, 10.22; N, 12.07; S, 9.21.

*4.2.2.2. Ethyl 2-(4-chloro-6-(4-chlorophenyl)-5-cyanopyrimidin-2-ylthio)acetate **(7g)***. Yield (64%), m.p. 166–169 °C. $\delta$ 1.05–1.13 (t, 3H, $CH_3$), 4.09–4.20 (m, 4H, $2CH_2$), 7.54–7.57(d, $J$ = 8.22 Hz 2H), 7.98–9.01(d, $J$ = 8.22 Hz, 2H). MS, *m/z* (%): 368(19%), 366(60%) for M+. Anal. Calcd for $C_{15}H_{11}Cl_2N_3O_2S$ (FW: 366): C, 48.93; H, 3.01; Cl, 19.26; N, 11.41; S, 8.71. Found: C, 48.77; H, 3.24; Cl, 19.00; N, 11.39; S, 8.82.

#### 4.2.3. Synthesis of compounds ***8a-c***

*4.2.3.1. Method A.* A solution of 4-hydroxybenzaldehyde (1.22 g, 10 mmol), potassium hydroxide (2.24 g, 40 mmol), triphenylphosphine (0.524 g, 2 mmol) and cupper (I) iodide (0.19 g, 1 mmol) in DMF (20 mL) was treated with compound **7a**, **7b** or **7c** (10 mmol). The reaction mixture was heated to 70 °C and stirred under Argon for 2 h. The reaction mixture was quenched with water and extracted with ethyl acetate. The organic extracts were dried ($Na_2SO4$), concentrated, and purified by column chromatography (0–25% EtOAc/n-hexane) to obtain yellow powders.

*4.2.3.2. 4-(4-formylphenoxy)-6-phenyl-2-thioxo-1,2-dihydropyrimidine-5-carbonitrile (8a)*. Yield (64%). m.p. 214–217 °C. $^1$H NMR (300 MHz, DMSO) 7.17–7.20(d, $J$ = 8.70 Hz, 2H), 7.33–7.37(m, 1H), 7.46–7.49(m, 2H), 7.69–7.71(m, 2H), 7.88–7.91(d, $J$ = 8.70 Hz, 2H), 10.03(s, 1H, CHO), 12.33(br., 1H, $D_2O$ exchangeable). MS, *m/z* (%): 333(M+, 24%). Anal. Calcd for $C_{18}H_{11}N_3O_2S$ (FW: 333): C, 64.85; H, 3.33; N, 12.60; S, 9.62. Found: C, 64.69; H, 3.50; N, 12.44; S, 9.75.

*4.2.3.3. Ethyl 2-(5-cyano-4-(4-fluorophenyl)-6-(4-formylphenoxy) pyrimidin-2-ylthio) acetate (8b).* Yield (64%), m.p. 153–155 °C. $^1$H NMR (300 MHz, DMSO) δ 1.02–1.07 (t, 3H), 3.92–3.99(m, 4H), 7.47–7.53(m, 2H), 7.57–7.60(d, *J* = 8.70 Hz, 2H), 8.05–8.11(m, 4H),10.07(s, 1H, CHO) . $^{13}$C NMR (75 MHz, DMSO) δ13.81, 33.32, 61.14, 114.22,115.87, 116.17, 122.46, 130.96, 131.32, 131.53, 131.64, 134.31, 155.66, 167.63, 167.90, 168.77, 192.00. MS, *m*/*z* (%): 437(M+, 24%). Anal. Calcd for $C_{22}H_{16}FN_3O_4S$ (FW: 437): C, 60.40; H, 3.69; F, 4.34; N, 9.61; S, 7.33. Found: C, 60.29; H, 3.65; N, 9.77; S, 7.42.

*4.2.3.4. 6-(4-Chlorophenyl)-4-(4-formylphenoxy)-2-thioxo-1,2-dihydropyrimidine-5-carbonitrile (8c).* Yield (64%), m.p. 244–247 °C. $^1$H NMR (300 MHz, DMSO) 7.33–7.37(d, *J* = 8.52 Hz, 2H), 7.44–7.47(d, *J* = 8.70 Hz, 2H), 7.89–7.91(d, *J* = 8.52 Hz, 2H), 8.02–8.05(d, *J* = 8.70 Hz, 2H), 10.07(s, 1H, CHO), 11.25(br., 1H, D2O exchangeable). MS, *m*/*z* (%): 367(M+, 28%). Anal. Calcd for $C_{18}H_{10}ClN_3O_2S$ (FW: 367): C, 58.78; H, 2.74; Cl, 9.64; N, 11.42; S, 8.72. Found: C, 58.55; H, 2.51; Cl, 9.44; N, 11.61; S, 8.97.

*4.2.4. Synthesis of compounds* ***9-a-c***

*4.2.4.1. Method B.* Compounds **8a-c** (10 mmol) were treated with a solution of 3,4-diaminobenzoic acid (1.53g, 10 mmol) in DMF (30 mL), followed by $Na_2S_2O_5$ (2.85g, 15 mmol). The mixture was heated to 90 °C for 24 h. The reaction mixture was cooled to room temperature then was quenched with water and the solid obtained was filtered and purified by column chromatography (0–100% EtOAc/n-hexane) to obtain yellow powders.

*4.2.4.2. 2-(4-(5-cyano-6-phenyl-2-thioxo-1,2-dihydropyrimidin-4-yloxy)phenyl)-1H-benzo[d]imidazole-5-carboxylic acid* ***(9a)***. Yield (64%), m.p. 262–265 °C. $^1$H NMR (300 MHz, DMSO) δ 7.27–7.35(m, 3H), 7.50–7.53(d, *J* = 8.70 Hz, 2H), 7.65–7.68(m, 2H), 7.70–7.73(d, *J* = 8.25 Hz, 1H), 7.88–7.91(d, *J* = 7.2 Hz, 1H), 8.23 (s, 1H), 8.32–8.35 (d, *J* = 8.70 Hz, 2H), 11.56 (br., 1H, $D_2O$ exchangeable), 12.69 (br., 1H, $D_2O$ exchangeable), 13.07 (br., 1H, $D_2O$ exchangeable). MS, *m*/*z* (%):465 (M+, 37%). Anal. Calcd for $C_{25}H_{15}N_5O_3S$ (FW: 465): C, 64.51; H, 3.25; N, 15.05; S, 6.89. Found: C, 64.32; H, 3.51; N, 15.21; S, 6.65.

*4.2.4.3. 2-(4-(5-cyano-2-(2-ethoxy-2-oxoethylthio)-6-(4-fluorophenyl)pyrimidin-4-yloxy) phenyl)-1H-benzo[d]imidazole-5-carboxylic acid* ***(9b)***. Yield (67%), m.p. 271–273 °C. $^1$H NMR (300 MHz, DMSO) δ 0.97–1.08 (t, 3H, $CH_3$), 3.92–4.08(m, 4H, $2CH_2$), 7.37–7.48(m, 2H), 7.50–7.53(d, *J* = 8.70 Hz, 2H), 7.70–7.73(d, *J* = 8.25 Hz, 1H), 7.88–7.91(d, *J* = 8.25 Hz, 1H), 8.05–8.08(m, 2H), 8.23 (s, 1H), 8.32–8.35 (d, *J* = 8.70 Hz, 2H), 10.56 (br., 1H, $D_2O$ exchangeable), 11.57(br., 1H, $D_2O$ exchangeable). $^{13}$C NMR (75 MHz, DMSO) δ 13.86, 33.35, 61.28, 110.29, 114.87, 115.87, 115.22, 116.29, 120.87, 122.33, 128.11, 129.32, 130.96, 131.32, 131.52, 131.64, 134.31, 147.52, 148.22, 149.22, 150.22, 152.47, 156.66, 167.03, 167.89, 168.44. MS, *m*/*z* (%): 569(M+, 38%). Anal. Calcd for $C_{29}H_{20}FN_5O_5S$ (FW: 569): C, 61.15; H, 3.54; F, 3.34; N, 12.30; S, 5.63. Found: C, 61.01; H, 3.39; N, 12.56; S, 5.77.

*4.2.4.4. 2-(4-(6-(4-chlorophenyl)-5-cyano-2-thioxo-1,2-dihydropyrimidin-4-yloxy)phenyl)-1H-benzo[d]imidazole-5-carboxylic acid* ***(9c)***. Yield (64%), m.p. 241–244 °C. $^1$H NMR (300 MHz, DMSO) 7.27–7.30(d, *J* = 8.52 Hz, 2H), 7.40–7.43(d, *J* = 8.70 Hz, 2H), 7.55–7.58(d, *J* = 8.52 Hz, 2H), 7.70–7.73(d, *J* = 8.25 Hz, 1H), 7.88–7.91(d, *J* = 8.25 Hz, 1H), 8.06 (s, 1H), 8.12–8.13(d, *J* = 8.70 Hz, 2H), 11.33 (br., 1H, $D_2O$ exchangeable), 13.07(br., 1H, D2O exchangeable). $^{13}$C NMR (75 MHz, DMSO) δ 113.77, 115.44, 115.22, 116.98, 120.87, 124.21, 125.61, 129.11, 130.66, 131.96, 131.52, 131.64, 138.31, 146.31, 148.22, 149.22, 150.22, 153.00, 156.66, 164.03, 166.40, 167.89, 168.44, 179.44. MS, *m*/*z* (%):499 (M+, 21%). Anal. Calcd for $C_{25}H_{14}ClN_5O_3S$ (FW: 499): C, 60.06; H, 2.82; Cl, 7.09; N, 14.01; S, 6.41. Found: C, 60.31; H, 2.75; Cl, 6.85; N, 14.31; S, 6.22.

*4.2.5. Synthesis of compounds* ***10a-c***

*4.2.5.1. Method C.* Compounds **9a-c** (10 mmol) were dissolved in DMF (20 mL), and 1,1-carbonyldiimidazole (0.16 g, 10 mmol) was added. The mixture was stirred for 30 min at room temperature and then cooled to 0 °C. Ammonium carbonate (0.19 g, 20 mmol) was added, and the reaction mixture was stirred for 24 h at room temperature. The solvent was evaporated under reduced pressure, and the residue quenched with water (30 mL) and extracted with ethyl acetate washed with water (3 × 50 mL), and dried (MgSO4). The organic extracts were then collected and concentrated. The residue was purified by column chromatography (0–100% EtOAc/n-hexane) and obtained as yellow powder.

*4.2.5.2. 2-(4-(5-cyano-6-phenyl-2-thioxo-1,2-dihydropyrimidin-4-yloxy)phenyl)-1H-benzo[d]imidazole-5-carboxamide* ***(10a)***. Yield (64%), m.p. 263–265 °C. $^1$H NMR (300 MHz, DMSO) δ 7.30–7.57(m, 5H), 7.66–7.69(m, 2H), 7.74–7.77(d, *J* = 8.25 Hz, 1H), 7.96–7.99(d, *J* = 8.25 Hz, 1H), 8.15 (s, 1H), 8.25–8.28 (d, *J* = 8.70 Hz, 2H), 8.54 (br., 2H, $D_2O$ exchangeable), 11.42, (br., 1H, $D_2O$ exchangeable). 13.01(br., 1H, $D_2O$ exchangeable). MS, *m*/*z* (%):465 (M+, 21%). Anal. Calcd for $C_{25}H_{16}N_6O_2S$ (FW: 464): C, 64.64; H, 3.47; N, 18.09; S, 6.90. Found: C, 64.68; H, 3.55; N, 17.94; S, 6.71.

*4.2.5.3. 2-(4-(5-cyano-2-(2-ethoxy-2-oxoethylthio)-6-(4-fluorophenyl)pyrimidin-4-yloxy) phenyl)-1H-benzo[d]imidazole-5-carboxamide* ***(10b)***. Yield (57%). m.p. 281–283 °C. $^1$H NMR (300 MHz, DMSO) δ 0.98–1.22 (t, 3H, $CH_3$), 3.99–4.21(m, 4H, $2CH_2$), 7.38–7.47(m, 2H), 7.50–7.53(d, *J* = 8.70 Hz, 2H), 7.69–7.72(d, *J* = 8.25 Hz, 1H), 7.88–7.91(d, *J* = 7.2 Hz, 1H), 8.01–8.12(m, 2H), 8.19 (s, 1H), 8.32–8.35 (d, *J* = 8.70 Hz, 2H), 8.69(br., 2H, $D_2O$ exchangeable), 11.31(br., 1H, NH, $D_2O$ exchangeable). MS, *m*/*z* (%): 568(M+, 22%). Anal. Calcd for $C_{29}H_{21}FN_6O_4S$ (FW: 568): C, 61.26; H, 3.72; F, 3.34; N, 14.78; S, 5.64. Found: C, 61.12; H, 3.57; N, 14.88; S, 5.80.

*4.2.5.4. 2-(4-(6-(4-chlorophenyl)-5-cyano-2-thioxo-1,2-dihydropyrimidin-4-yloxy)phenyl)-1H-benzo[d]imidazole-5-carboxamide* ***(10c)***. Yield (61%). m.p. 278–280 °C. $^1$H NMR (300 MHz, DMSO) 7.21–7.24(d, *J* = 8.70 Hz, 2H), 7.43–7.46 (d, *J* = 8.52 Hz, 2H), 7.63–7.66 (d, *J* = 8.52 Hz, 2H), 7.78–7.81 (d, *J* = 8.20 Hz, 1H), 8.08–8.11 (d, *J* = 8.20 Hz, 1H), 8.26 (s, 1H), 8.32–8.35 (d, *J* = 8.70 Hz, 2H), 8.64 (br., 2H, $D_2O$ exchangeable), 11.68 (br., 1H, $D_2O$ exchangeable), 13.09 (br., 1H, $D_2O$ exchangeable). MS, *m*/*z* (%):498 (M+, 27%), 500(M+, 8%). Anal. Calcd for $C_{25}H_{15}ClN_6O_2S$ (FW: 498): C, 60.18; H, 3.03; Cl, 7.11; N, 16.84; S, 6.43. Found: C, 60.02; H, 3.22; Cl, 7.04; N, 16.77; S, 6.56.

*4.2.6. Synthesis of compounds* ***11a-f***

*4.2.6.1. 4-(5-Cyano-6-(4-nitrophenyl)-2-thioxo-1,2-dihydropyrimidin-4-ylamino)benzoic acid* ***(11a)***. Prepared according to method (A) by reaction of 4-chloro-6-(4-nitrophenyl)-2-thioxo-1,2-dihydropyrimidine-5-carbonitrile (**7d**) with 4-aminobenzoic acid. Yield (57%). m.p. 259–262 °C. $^1$H NMR (300 MHz, DMSO) 4.52 (br., 1H, $D_2O$ exchangeable), 7.24–7.27(d, *J* = 8.70 Hz, 2H), 7.85–7.89(d, *J* = 8.52 Hz, 2H), 8.09–8.11(d, *J* = 8.52 Hz, 2H), 8.32–8.35(d, *J* = 8.70 Hz, 2H), 12.74 (br., 1H, $D_2O$ exchangeable) 13.25 (br., 1H, $D_2O$ exchangeable). MS, *m*/*z* (%): 393(M+, 28%). Anal. Calcd for $C_{18}H_{11}N_5O_4S$ (FW: 393): C, 54.96; H, 2.82; N, 17.80; S, 8.15. Found: C, 54.78; H, 2.97; N, 17.69; S, 8.27.

*4.2.6.2. 4-(5-Cyano-6-(4-methoxyphenyl)-2-thioxo-1,2-dihydropyrimidin-4-ylamino)benzoic acid* ***(11b)***. Prepared according

to method (A) by reaction of 4-chloro-6-(4-methoxyphenyl)-2-thioxo-1,2-dihydropyrimidine-5-carbonitrile(**7e**) with 4-aminobenzoic acid. Yield (42%). m.p. 271–274 °C. $^1$H NMR (300 MHz, DMSO) 3.83 (s, 3H), 5.22 (br., 1H, $D_2O$ exchangeable), 7.06–7.09 (d, $J = 8.64$ Hz, 2H), 7.37–7.40(d, $J = 8.52$ Hz, 2H), 7.59–7.61(d, $J = 8.52$ Hz, 2H), 7.82–7.85(d, $J = 8.64$ Hz, 2H), 12.44 (br., 1H, $D_2O$ exchangeable) 12.94 (br., 1H, $D_2O$ exchangeable). MS, *m/z* (%): 378(M+, 28%). Anal. Calcd for $C_{19}H_{14}N_4O_3S$ (FW: 378): C, 60.31; H, 3.73; N, 14.81; S, 8.47. Found: C, 60.48; H, 3.66; N, 14.94; S, 8.61.

*4.2.6.3. 4-(5-Cyano-6-(4-methoxyphenyl)-2-thioxo-1,2-dihydropyrimidin-4-ylthio)benzoic acid* ***(11c)***. Prepared according to method (A) by reaction of 4-chloro-6-(4-methoxyphenyl)-2-thioxo-1,2-dihydropyrimidine-5-carbonitrile (**7e**) with 4-mercaptobenzoic acid. Yield (42%). m.p. 283–285 °C. $^1$H NMR (300 MHz, DMSO) $\delta$ 3.82 (s, 3H), 7.16–7.19 (d, $J = 8.64$ Hz, 2H), 7.57–7.60 (d, $J = 8.52$ Hz, 2H), 7.68–7.71 (d, $J = 8.52$ Hz, 2H), 8.02–8.05 (d, $J = 8.64$ Hz, 2H), 12.74 (br., 1H, $D_2O$ exchangeable) 13.52 (br., 1H, $D_2O$ exchangeable). MS, *m/z* (%): 395(M+, 42%). Anal. Calcd for $C_{19}H_{13}N_3O_3S_2$ (FW: 395): C, 57.71; H, 3.31; N, 10.63; S, 16.22. Found: C, 57.65; H, 3.22; N, 10.71; S, 16.09.

*4.2.6.4. 4-(5-Cyano-2-thioxo-6-p-tolyl-1,2-dihydropyrimidin-4-ylthio)benzoic acid* ***(11d)***. Prepared according to method (A) by reaction of 4-chloro-6-*p*-tolyl-2-thioxo-1,2-dihydropyrimidine-5-carbonitrile (**7f**) with 4-mercaptobenzoic acid. Yield (51%), m.p. 252–254 °C. $^1$H NMR (300 MHz, DMSO) $\delta$ 2.31 (s, $CH_3$), 7.16–7.19 (d, $J = 8.64$ Hz, 2H), 7.27–7.30(d, $J = 8.33$ Hz, 2H), 7.66–7.69 (d, $J = 8.52$ Hz, 2H), 8.08–8.11 (d, $J = 8.52$ Hz, 2H), 12.79 (br., 1H, $D_2O$ exchangeable) 13.10 (br., 1H, $D_2O$ exchangeable). MS, *m/z* (%): 379(M+, 40%). Anal. Calcd for $C_{19}H_{13}N_3O_2S_2$ (FW: 379): C, 60.14; H, 3.45; N, 11.07; S, 16.90. Found: C, 60.02; H, 3.22; N, 11.31; S, 16.74.

*4.2.6.5. 4-(6-(4-Chlorophenyl)-5-cyano-2-thioxo-1,2-dihydropyrimidin-4-ylthio)benzoic acid* ***(11e)***. Prepared according to method (A) by reaction of 4-chloro-6-(4-Chlorophenyl)-2-thioxo-1,2-dihydropyrimidine-5-carbonitrile (**7c**) with 4-mercaptobenzoic acid. Yield (62%), m.p. 274–277 °C. $^1$H NMR (300 MHz, DMSO) $\delta$ 7.35–7.38 (d, $J = 8.50$ Hz, 2H), 7.48–7.51(d, $J = 8.50$ Hz, 2H), 7.65–7.68(d, $J = 8.48$ Hz, 2H), 8.08–8.11 (d, $J = 8.48$ Hz, 2H), 12.55 (br., 1H, $D_2O$ exchangeable) 13.37 (br., 1H, $D_2O$ exchangeable). MS, *m/z* (%):399 (M+, 28%), 401(M+, 9%) 28%). Anal. Calcd for $C_{18}H_{10}ClN_3O_2S_2$ (FW: 398.99): C, 54.07; H, 2.52; Cl, 8.87; N, 10.51; S, 16.04. Found: C, 53.89; H, 2.34; Cl, 8.66; N, 10.64; S, 16.12.

*4.2.6.6. 4-(6-(4-chlorophenyl)-5-cyano-2-(2-ethoxy-2-oxoethylthio) pyrimidin-4-ylthio)benzoic acid* ***(11f)***. Prepared according to method (A) by reaction of 4-chloro-6-(4-Chlorophenyl)-2-(2-ethoxy-2-oxoethylthio)-1,2-dihydropyrimidine-5-carbonitrile (**7g**) with 4-mercaptobenzoic acid. Yield (54%), m.p. 264–267 °C. $^1$H NMR (300 MHz, DMSO) $\delta$ 1.08–1.22 (t, 3H, $CH_3$), 4.03–4.21(m, 4H, $2CH_2$), 2H), 7.55–7.759(m, 4H), 7.82–7.85(d, $J = 8.24$ Hz, 2H), 8.01–8.04(d, $J = 8.52$ Hz, 2H), 12.50 (br., 1H, $D_2O$ exchangeable). MS, *m/z* (%): 485 (M+, 31%), 487 (M+, 11%). Anal. Calcd for $C_{22}H_{16}ClN_3O_4S_2$ (FW: 485): C, 54.37; H, 3.32; Cl, 7.30; N, 8.65; S, 13.20. Found: C, 54.54; H, 3.49; Cl, 7.14; N, 8.57; S, 13.41.

*4.2.7. Synthesis of compounds* ***12***, ***13*** *and* ***16–19***

*4.2.7.1. Method D.* Compounds **11a-f** (10 mmol) were treated with a solution of 3,4-diaminobenzoic acid (1.53g, 10 mmol) in polyphosphoric acid (20 mL). The mixture was heated to 150–180 °C for 4 h. The reaction mixture was cooled to room temperature then was quenched with water and neutralized with $NH_4OH$ the solid was filtered and was purified by column chromatography (0–100% EtOAc/n-hexane).

*4.2.7.2. 2-(4-(5-cyano-6-(4-nitrophenyl)-2-thioxo-1,2-dihydropyrimidin-4-ylamino)phenyl)-1H-benzo[d]imidazole-5-carboxylic acid* ***(12)***. Prepared by reaction of compound **11a** with 3,4-diaminobenzoic acid according to method **D.** Yield (28%), m.p. 305–307 °C. $^1$H NMR (300 MHz, DMSO) $\delta$ 5.65 (s., 1H, $D_2O$ exchangeable), 7.17–7.19 (d, $J = 8.36$ Hz, 2H), 7.64–7.66 (d, $J = 8.12$ Hz, 1H), 7.72–7.74(d, $J = 8.36$ Hz, 2H), 7.82–7.84 (d, $J = 8.12$ Hz, 1H), 7.92–7.94 (d, $J = 8.36$ Hz, 2H), 8.20 (s, 1H), 8.38–8.40(d, $J = 8.36$ Hz, 2H), 12.04 (s., 1H, $D_2O$ exchangeable), 12.15 (s., 1H, $D_2O$ exchangeable), 12.75(br., 1H, $D_2O$ exchangeable). MS, *m/z* (%):509 (M+, 45%). Anal. Calcd for$C_{25}H_{15}N_7O_4S$ (FW: 509): C, 58.93; H, 2.97; N, 19.24; S, 6.29. Found: C, 58.71; H, 2.68; N, 19.55; S, 6.42.

*4.2.7.3. 2-(4-(5-cyano-6-(4-methoxyphenyl)-2-thioxo-1,2-dihydropyrimidin-4-ylamino)phenyl)-1H-benzo[d]imidazole-5-carboxylic acid****(13)***. Prepared by reaction of compound **11b** with 3,4-diaminobenzoic acid according to method **D.** Yield (25%), m.p. 287–289 °C. $^1$H NMR (300 MHz, DMSO) δ3.81 (s, 3H), 5.24 (br., 1H, $D_2O$ exchangeable), 7.05–7.08(d, $J = 8.35$ Hz, 2H), 7.22–7.25(d, $J = 8.25$ Hz, 2H), 7.66–7.69(d, $J = 8.35$ Hz, 2H), 7.88–7.91(m, 3H), 8.15–8.18(d, $J = 8.35$ Hz, 1H), 8.23 (s, 1H), 11.43 (br., 1H, $D_2O$ exchangeable), 12.55 (br., 1H, $D_2O$ exchangeable), 13.33(br., 1H, $D_2O$ exchangeable). $^{13}$C NMR (75 MHz, DMSO) $\delta$ 58.32, 115.17, 116.12, 116.54, 119.84, 120.87, 124.21, 125.61, 129.33, 129.98, 131.96, 131.46, 133.20, 139.01, 146.31, 147.27, 148.31, 150.75, 152.52, 159.24, 163.99, 165.24, 166.87, 181.07. MS, *m/z* (%):494 (M+, 45%). Anal. Calcd for-$C_{26}H_{18}N_6O_3S$ (FW: 494): C, 63.15; H, 3.67; N, 16.99; S, 6.48. Found: C, 63.25; H, 3.70; N, 16.81; S, 6.66.

*4.2.7.4. 2-(4-(5-cyano-6-(4-methoxyphenyl)-2-thioxo-1,2-dihydropyrimidin-4-ylthio)phenyl)-1H-benzo[d]imidazole-5-carboxylic acid* ***(16)***. Prepared by reaction of compound **11c** with 3,4-diaminobenzoic acid according to method **D.** Yield (27%), m.p. 301–303 °C. $^1$H NMR (300 MHz, DMSO) δ3.81 (s, 3H), 7.01–7.04(d, $J = 8.25$ Hz, 2H), 7.46–7.49(m, 4H), 7.73–7.77(d, $J = 8.25$ Hz, 2H), 7.85–7.88(d, $J = 8.35$ Hz, 1H), 8.09–8.12(d, $J = 8.35$ Hz, 1H), 8.23 (s, 1H), 11.61 (br., 1H, $D_2O$ exchangeable), 12.89 (br., 1H, $D_2O$ exchangeable), 13.03(br., 1H, $D_2O$ exchangeable). MS, *m/z* (%): 511 (M+, 31%). Anal. Calcd for$C_{26}H_{17}N_5O_3S_2$ (FW: 511): C, 61.04; H, 3.35; N, 13.69; S, 12.54. Found: C, 61.22; H, 3.41; N, 13.48 S, 12.33.

*4.2.7.5. 2-(4-(5-cyano-2-thioxo-6-p-tolyl-1,2-dihydropyrimidin-4-ylthio)phenyl)-1H-benzo[d]imidazole-5-carboxylic acid* ***(17)***. Prepared by reaction of compound **11d** with 3,4-diaminobenzoic acid according to method **D.** Yield (27%), m.p. 265–267 °C. $^1$H NMR (300 MHz, DMSO) δ2.33 (s, 3H), 7.12–7.15(d, $J = 8.26$ Hz, 2H), 7.46–7.49(d, $J = 8.25$ Hz, 2H), 7.68–7.71(d, $J = 8.36$ Hz, 2H), 7.80–7.83(d, $J = 8.36$ Hz, 2H), 7.91–7.94(d, $J = 8.35$ Hz, 1H), 8.05–8.08(d, $J = 8.35$ Hz, 1H), 8.21 (s, 1H), 11.61 (br., 1H, $D_2O$ exchangeable), 12.78 (br., 1H, $D_2O$ exchangeable), 13.22 (br., 1H, $D_2O$ exchangeable). MS, *m/z* (%): 495 (M+, 45%). Anal. Calcd for-$C_{26}H_{17}N_5O_2S_2$ (FW: 495): C, 63.01; H, 3.46; N, 14.13; S, 12.94. Found: C, 63.22; H, 3.59; N, 14.21; S, 13.09.

*4.2.7.6. 2-(4-(6-(4-chlorophenyl)-5-cyano-2-thioxo-1,2-dihydropyrimidin-4-ylthio)phenyl)-1H-benzo[d]imidazole-5-carboxylic acid* ***(18)***. Prepared by reaction of compound **11e** with 3,4-diaminobenzoic acid according to method **D.** Yield (25%), m.p. 322–324 °C. $^1$H NMR (400 MHz, DMSO) $\delta$ 7.27–7.29(d, $J = 8.36$ Hz, 2H), 7.55–7.57 (d, $J = 8.32$ Hz, 2H), 7.63–7.65(d, $J = 8.36$ Hz, 1H), 7. 74-7. 76 (d, $J = 8.$ 36 Hz, 2H), 7.91–7.93(d, $J = 8.36$ Hz, 1H), 8.01–8.03(d, $J = 8.36$ Hz, 1H), 8.22 (s, 1H), 12.04 (s., 1H, $D_2O$

exchangeable), 12.16 (s., 1H, $D_2O$ exchangeable), 12.75 (br., 1H, $D_2O$ exchangeable). $^{13}C$ NMR (75 MHz, DMSO) $\delta$ 114.69, 114.99, 116.30, 117.50, 123.38, 124.22, 124.59, 125.16, 125.46, 129.26, 133.30, 135.43, 137.70, 140.45, 144.21, 154.95, 155.28, 161.73, 166.58, 167.77, 180.05. MS, *m/z* (%): 515 (M+, 39%), 517 (M+, 14%). Anal. Calcd for $C_{25}H_{14}ClN_5O_2S_2$ (FW: 515): C, 58.19; H, 2.73; Cl, 6.87; N, 13.57; S, 12.43. Found: C, 58.31; H, 2.97; Cl, 6.56; N, 13.32; S, 12.54.

*4.2.7.7. 2-(4-(6-(4-chlorophenyl)-5-cyano-2-(2-ethoxy-2-oxoethylthio) pyrimidin-4-ylthio)phenyl)-1H-benzo[d]imidazole-5-carboxylic acid* ***(19)***. Prepared by reaction of compound **11f** with 3,4-diaminobenzoic acid according to method D.

$^1H$ NMR (300 MHz, DMSO) $\delta$ 1.18–1.29 (t, 3H, $CH_3$), 4.02–4.18(m, 4H, $2CH_2$), 7.48–7.51(d, $J = 8.25$ Hz, 2H), 7.62–7.65 (d, $J = 8.35$ Hz, 2H), 7.72–7.75(d, $J = 8.35$ Hz, 2H), 7.83–7.86 (d, $J = 8.25$ Hz, 1H), 7.96–7.99 (d, $J = 8.35$ Hz, 2H), 8.15–8.18 (d, $J = 8.22$ Hz, 1H), 8.25 (s, 1H), 11.56 (br., 1H, $D_2O$ exchangeable), 12.75 (br., 1H, $D_2O$ exchangeable). MS, *m/z* (%): 601(M+, 25%), 603(M+, 8%). Anal. Calcd for $C_{29}H_{20}ClN_5O_4S_2$ (FW: 601): C, 57.85; H, 3.35; Cl, 5.89; N, 11.63; S, 10.65. Found: C, 57.67; H, 3.29; Cl, 5.77; N, 11.42; S, 10.72.

### *4.2.8. Synthesis of compounds* ***14***, ***15*** *and* ***20–23***

*4.2.8.1. 2-(4-(5-cyano-6-(4-nitrophenyl)-2-thioxo-1,2-dihydropyrimidin-4-ylamino)phenyl)-1H-benzo[d]imidazole-5-carboxamide* ***(14)***. Prepared by the reaction of compound **12** with ammonium carbonate according to method **C.** Yield (68%), m.p. 291–293 °C. $^1H$ NMR (400 MHz, DMSO) $\delta$ 5.53–5.58 (br., 1H, $D_2O$ exchangeable), 7.24–7.26(d, $J = 8.36$ Hz, 2H), 7.76–7.78(d, $J = 8.36$ Hz, 1H), 7.94–7.96(d, $J = 8.$ 44 Hz, 2H), 7.97–7.99(m, 3H), 8.14 (s, 1H), 8.21–8.23(d, $J = 8.44$ Hz, 2H), 8.51–8.55 (br., 2H, $D_2O$ exchangeable), 12.17 (br., 1H, $D_2O$ exchangeable), 12.37 (br., 1H, $D_2O$ exchangeable). MS, *m/z* (%):508 (M+, 24%). Anal. Calcd for- $C_{25}H_{16}N_8O_3S$ (FW: 508): C, 59.05; H, 3.17; N, 22.04; S, 6.31. Found: C, 59.31; H, 3.25; N, 22.13; S, 6.19.

*4.2.8.2. 2-(4-(5-cyano-6-(4-methoxyphenyl)-2-thioxo-1,2-dihydropyrimidin-4-ylamino)phenyl)-1H-benzo[d]imidazole-5-carboxamide* ***(15)***. Prepared by reaction of compound **13** with ammonium carbonate according to method **C.** Yield (67%), m.p. 318–320 °C. $^1H$ NMR (400 MHz, DMSO) $\delta$3.85 (s, 3H), 5.09 (br., 1H, $D_2O$ exchangeable), 6.94–6.96 (d, $J = 8.24$ Hz, 2H), 7.26–7.28(d, $J = 8.36$ Hz, 2H), 7.65–7.67(d, $J = 8.24$ Hz, 2H), 7.72–7.74(d, $J = 8.32$ Hz, 1H), 7.88–7.90(d, $J = 8.36$ Hz, 2H), 7.95–7.97 (d, $J = 8.32$ Hz, 1H), 8.13 (s, 1H), 8.61–8.65 (br., 2H, $D_2O$ exchangeable), 12.17 (br., 1H, $D_2O$ exchangeable), 12.37 (br., 1H, $D_2O$ exchangeable). MS, *m/z* (%):493 (M+, 34%). Anal. Calcd for $C_{26}H_{19}N_7O_2S$ (FW: 493): C, 63.27; H, 3.88; N, 19.87; S, 6.50. Found: C, 63.50; H, 3.77; N, 19.67; S, 6.39.

*4.2.8.3. 2-(4-(5-cyano-6-(4-methoxyphenyl)-2-thioxo-1,2-dihydropyrimidin-4-ylthio)phenyl)-1H-benzo[d]imidazole-5-carboxamide* ***(20)***. Prepared by the reaction of compound **16** with ammonium carbonate according to method **C.** Yield (60%), m.p, 325–327 °C. $^1H$ NMR (300 MHz, DMSO) $\delta$3.81 (s, 3H), 7.03–7.06 (d, $J = 8.35$ Hz, 2H), 7.43–7.46(d, $J = 8.70$ Hz, 2H), 7.60–7.63(d, $J = 8.35$ Hz, 2H), 7.76–7.79(d, $J = 8.70$ Hz, 2H), 7.93–7.96(d, $J = 8.20$ Hz, 1H), 8.04–8.07(d, $J = 8.20$ Hz, 1H), 8.23 (s, 1H), 8.69 (br., 2H, $D_2O$ exchangeable), 12.47 (br., 1H, $D_2O$ exchangeable), 13.21(br., 1H, $D_2O$ exchangeable). $^{13}C$ NMR (75 MHz, DMSO) $\delta$ 55.99. 115.03, 115.92, 116.44, 121.17, 122.47, 123.66, 127.42, 127.89, 129.41, 130.11, 132.42, 134.55, 139.65, 144.89, 152.67, 160.99. 162.69, 163.41, 168.09, 180.13. MS, *m/z* (%): 510 ($M^+$, 16%). Anal. Calcd for $C_{26}H_{18}N_6O_2S_2$ (FW: 510): C, 61.16; H, 3.55; N, 16.46; S, 12.56. Found: C, 61.01; H, 3.42; N, 16.33; S, 12.72.

*4.2.8.4. 2-(4-(5-cyano-2-thioxo-6-p-tolyl-1,2-dihydropyrimidin-4-ylthio)phenyl)-1H-benzo[d]imidazole-5-carboxamide* ***(21)***. Prepared by reaction of compound **17** with ammonium carbonate according to method **C.** Yield (27%), m.p. 299–302 °C. $^1H$ NMR (300 MHz, DMSO) $\delta$2.33 (s, 3H), 7.12–7.13(d, $J = 8.25$ Hz, 2H), 7.24–7.27(d, $J = 8.25$ Hz, 2H), 7.46–7.49(d, $J = 8.70$ Hz, 2H), 7.68–7.71(d, $J = 8.70$ Hz, 2H), 7.91–7.94(d, $J = 8.25$ Hz, 1H), 8.05–8.08(d, $J = 8.25$ Hz, 1H), 8.21 (s, 1H), 8.61 (br., 2H, $D_2O$ exchangeable), 12.78 (br., 1H, $D_2O$ exchangeable), 13.22 (br., 1H, $D_2O$ exchangeable). $^{13}C$ NMR (75 MHz, DMSO) $\delta$ 21.59, 115.45, 116.3117.21, 122.34, 124.98, 127.49, 128.71, 128.99, 129.44, 130.10, 131.11, 134.58, 137.66, 140.21, 145.34, 152.13, 163.33, 164.03, 168.00, 180.27. MS, *m/z* (%): 494 ($M^+$, 45%). Anal. Calcd for $C_{26}H_{18}N_6OS_2$ (FW: 494): C, 63.14; H, 3.67; N, 16.99; S, 12.97. Found: C, 63.14; H, 3.67; N, 16.99; S, 12.97.

*4.2.8.5. 2-(4-(6-(4-chlorophenyl)-5-cyano-2-thioxo-1,2-dihydropyrimidin-4-ylthio)phenyl)-1H-benzo[d]imidazole-5-carboxamide* ***(22)***. Prepared by reaction of compound **18** with ammonium carbonate according to method **C.** Yield (25%), m.p. 330–332 °C. $^1H$ NMR (300 MHz, DMSO) $\delta$7.22–7.25(d, $J = 8.70$ Hz, 2H), 7.33–7.51(m, 4H), 7.65–7.68(d, $J = 8.70$ Hz, 2H), 7.91–7.94(d, $J = 8.25$ Hz, 1H), 8.08–8.11(d, $J = 8.25$ Hz, 1H), 8.21 (s, 1H), 8.65 (br., 2H, $D_2O$ exchangeable), 12.49 (br., 1H, $D_2O$ exchangeable), 13.08 (br., 1H, $D_2O$ exchangeable). $^{13}C$ NMR (75 MHz, DMSO) $\delta$ 115.22, 115.55, 116.54, 120.74, 122.20, 127.41, 127.87, 128.47, 129.82, 130.10, 131.87, 135.32, 135.55, 139.24, 145.90, 152.74, 163.04, 163.49, 168.11, 180.55. MS, *m/z* (%): 514 (M+, 24% for $Cl^{35.5}$), 516 (M+, 10% for $Cl^{37.5}$). Anal. Calcd for $C_{25}H_{15}ClN_6OS_2$ (FW: 514): C, 58.30; H, 2.94; Cl, 6.88; N, 16.32; S, 12.45. Found: C, 58.48; H, 2.77; Cl, 6.64; N, 16.45; S, 12.61.

*4.2.8.6. 2-(4-(6-(4-chlorophenyl)-5-cyano-2-(2-ethoxy-2-oxoethylthio) pyrimidin-4-ylthio) phenyl)-1H-benzo[d]imidazole-5-carboxamide* ***(23)***. Prepared by the reaction of compound **19** with ammonium carbonate according to method **C**. Yield (28%), m.p. 317–320 °C. $^1H$ NMR (300 MHz, DMSO) $\delta$ 1.21–1.29 (t, 3H, $CH_3$), 4.04–4.18(m, 4H, $2CH_2$), 7.40–7.43(d, $J = 8.25$ Hz, 2H), 7.52–7.55(d, $J = 8.70$ Hz, 2H), 7.67–7.70(d, $J = 8.25$ Hz, 2H), 7.87–7.90(d, $J = 8.20$ Hz, 1H), 7.97–8.00(d, $J = 8.70$ Hz, 2H), 8.12–8.15(d, $J = 8.20$ Hz, 1H), 8.23 (s, 1H), 8.55 (br., 2H, $D_2O$ exchangeable), 12.71(br., 1H, $D_2O$ exchangeable). $^{13}C$ NMR (75 MHz, DMSO) $\delta$14.12, 35.46, 60.54, 100.44, 115.20, 116.87, 117.31, 122.34, 127.44, 127.65, 127.72, 128.78, 129.83, 129.99, 131.20, 131.68, 133.49, 134.09, 139.54, 145.63, 152.44, 164.47, 168.21, 169.87, 176.55, 192.21. MS, *m/z* (%): 600($M^+$, 39% for $Cl^{35.5}$), 602($M^+$, 16% for $Cl^{37.5}$). Anal. Calcd. for- $C_{29}H_{21}ClN_6O_3S_2$ (FW: 600): C, 57.95; H, 3.52; Cl, 5.90; N, 13.98; S, 10.67. Found: C, 57.79 H, 3.33; Cl, 5.87; N, 14.08; S, 10.81.

### *4.3. In vitro checkpoint Kinase Assay*

The CycLex® Checkpoint Kinase Assay/Inhibitor Screening Kit was used to measure the activities of checkpoint kinases by using a phospho-Cdc25C (Ser216) monoclonal antibody to provide a specific and sensitive method. Chk2 positive control (CY-E1162-2) was used. Assay conditions were based on published protocols with minor modifications. The optical density (O.D.) of each well was measured using a spectrophotometric plate reader at dual wavelengths of 450/492 nm using ELISA microplate reader. Then, assays were repeated by using mixture of optimum concentration of positive control that exhibited maximum activity of checkpoint kinase 2 (0.01 unit/well) and specific concentration of each compound A = 2.5 μmol/l, B = 1.5 μmol/L, C = 0.1 μmol/L, D = 0.050 μmol/L and E = 0.025 μmol/L. The $IC_{50}$ (concentration that produces 50% of enzyme inhibition) by synthesized compounds as Chk2 inhibitors has been calculated as the mean value of

at four replicate experiments. %inhibition= (1-(OD of the compound at specific conc. − OD of negative control)÷ (OD of pos. control - OD of negative control)) X100, (All data are represented in supplementary material).

### 4.4. Western blot

MCF-7 breast carcinoma including untreated cells (control cells), treated cells with $GI_{50}$ of compound 8, **9**, $GI_{50}$ of cisplatin alone or $GI_{50}$ of cisplatin in combination with 0.1 μM of compound 8, **9.** Cells were grown to ~70% confluency and reagents were added as indicated concentrations. Cells were lysed in lysis buffer containing Tris-HCl (20 mM), NaCl (0.5 M), Triton X-100(0.25%), EDTA (1 mM), EGTA, (1 mM), glycophosphate (10 mM), NaF (10 mM), $Na_3VO_4$ (300 lM), benzamidine (1 mM), PMSF (2 lM) and DTT (1 mM). The protein concentration was determined by the BCA protein assay (Thermo Scientific, Rockford, IL, USA). Proteins were separated on SDS-PAGE, transferred on to nitrocellulose membrane (NC). NC sheets were cut into 0.5 cm strips [52]. Followed by blocking in 5% dry skimmed milk in TBS-T for 2 h on rocker platform and then, following washing by TBS-T. The strips were probed with phosphorylated anti-Chk2 antibody (Sigma-Aldrich) in 1:200 concentrations. Anti-mouse IgM peroxidase (Sigma-Aldrich) diluted at 1: 1000 in TBS was added to NC strips for 1 h on a rocker platform, The *o*-phenylene diamine tablet (Sigma-Aldrich) dissolved in 10 mL methanol and completed to 50 mL with TBS was added to NC stripes for 30 min [53].

Immunoreactivity was detected using the ECL detection system (Amersham Biosciences).

### 4.5. Cytotoxicity assay

#### 4.5.1. Cell lines

Breast carcinoma, estrogen receptor positive (ER+) cell line (MCF-7) was used in this study. It was obtained frozen in liquid nitrogen (−180 °C) from the American Type Culture Collection (ATTC, USA). The tumor cell lines were maintained by serial sub culturing at the National Cancer Institute, Cairo, Egypt. They were cultured in RPMI-1640 medium supplemented with 10% fetal bovine serum, 100 U/ml penicillin, 100 mg/mL streptomycin, and 3 mM glutamine and incubated in humidified incubator at 37 °C and 5% $CO_2$. The cells were sub-cultured every three days. Cisplatin and doxorubicin were purchased from Sigma Chemical Co. (St. Louis, MO, USA). The cytotoxicity of the synthesized compounds in addition to two reference compounds (positive control) cisplatin and doxorubicin were tested on MCF7 cancer cell lines, using sulphorhodamine-B (SRB) method [46]. In brief; cells were seeded at a density of $3 \times 10^3$ cells/well in 96-well microliter plates. They were left to attach for 24 h before incubation with studied compounds or drugs. Then, cells were treated with different concentrations of the Chk2 inhibitors (0.05, 0.1, 0.15 and 0.2 μmol). For each concentration, three wells were used and incubation was continued for 48 h. A negative control well-containing solvent as DMSO its concentration does not exceed (1% v/v) was included. At the end of incubation, cells were fixed with 20% trichloroacetic acid (TCA), stained with 0.4% SRB dye. The optical density (O.D.) of each well was measured spectrophotometrically at 570 nm using ELISA microplate reader (TECAN sunrise™, Germany). The mean survival fraction at each drug concentration was calculated as follows: O.D. of the treated cells/O.D. of the control cells. The $GI_{50}$ (concentration that produces 50% of cell growth inhibition) value of each drug was calculated using sigmoidal dose response curve fitting models (Graph Pad Prizm software, version 5). Each value is the mean ± SD of 5 independent experiments performed in triplicates; the surviving fraction = O.D. (treated cells)/O.D. (control cells).

The statistical significance of the results was analyzed using one-way ANOVA followed by Tukey multiple comparison tests.

#### 4.5.2. Combined effect of different concentrations of the tested compounds and $IG_{50}$ of cisplatin or doxorubicin on MCF7

The combination regimens were designed using $GI_{50}$ of doxorubicin and cisplatin with different concentrations of Chk2 inhibitors on MCF-7 cells. Different concentrations of the studied compounds were chosen to test their combination with doxorubicin and cisplatin for further experiments. MCF7 was plated in 96 well plates at concentration $3 \times 10^3$ cells/well and were left to attach for 24 h before incubation with drugs. MCF7 cells were treated with either $GI_{50}$ of doxorubicin or cisplatin alone and with different concentrations of the Chk2 inhibitors (0.05, 0.1, 0.15 and 0.2 μmol) and incubated for 48 h. At the end of incubation, cells were fixed with 20% trichloroacetic acid (TCA) and stained with 0.4% SRB dye as previously described [46].

### 4.6. Propidium iodide staining

Cells were plated in 60-mm dishes at $2 \times 10^5$ cells/mL RPMI. On the following day, the cells were treated with $GI_{50}$ of cisplatin, compound **8** or **9** alone or combination of $GI_{50}$ of cisplatin with 0.1 μM of synthesized conjugates **8** or **9** for 48 h, fixed with 2% paraformaldehyde solution, and incubated with propidium iodide buffer (0.1% sodium citrate, 0.1% Triton X-100, and 0.1 mg/mL propidium iodide). Subsequently, nuclei of the cells were observed with confocal microscope (Zeiss LSM 710), the objective lens is 20X, the cells were counted in 5 points of dimension 1700 $\mu m^2$ magnification 200X.

### 4.7. Cell cycle analysis

Briefly cell cycle phase modifications were examined by flow on propidium iodide–stained cells using Cycle TEST™ PLUS DNA Reagent (BECTON DICKINSON, San Jose, California, U.S.A.) that was used following the manufacturer's protocol, including that for staining with propidium iodide for cell-cycle analysis on MCF-7 cells that treated with DMSO or with either $GI_{50}$ of doxorubicin alone, and with 0.1 μM or with $GI_{50}$ of studied compounds as previously described [46]. Cells were analyzed by flow cytometry to quantify the numbers of apoptotic cells and the distribution of cells throughout the cell cycle.

In conclusion, our synthesized compounds demonstrated strong antitumor activity alone and in combination with other genotoxic drugs as cisplatin and doxorubicin via inhibition of Chk2, induction of apoptosis and cell cycle arrest.

## Acknowledgements

We gratefully acknowledge the financial support of Science and Technology Development Fund, Egypt (STDF) administered through Basic and Applied Research Grants (Grant number ID: STDF 3130) to Dr. Shadia A. Galal and we deeply thank Prof. Dr. Maha A. El-Demellawy for valuable comments and advises along the project. Authors also thank the staff members of “Embryo and genetic resources conservation bank” in National Research Centre for using Confocal microscope (Zeiss LSM 710) in apoptotic analysis that was administered by STDF grant number (STDF-CB, ID: 2339) and STDF-RSDTG project of grant number ID: 6901 to Prof. Dr. Omaima M. Kandil (Email: omaima_mk@yahoo.com).

## Appendix A. Supplementary data

Supplementary data related to this article can be found at https://doi.org/10.1016/j.ejmech.2018.01.072.

## References


[1] L.M. Coussens, Z. Werb, Inflammation and cancer, Nature 420 (2002) 860–867.
[2] S.I. Grivennikov, F.R. Greten, M. Karin, Immunity, inflammation, and cancer, Cell 140 (2010) 883–899.
[3] V. Shafirovich, N.E. Geacintov, Removal of oxidatively generated DNA damage by overlapping repair pathways, Free Radic. Biol. (2016), https://doi.org/10.1016/j.freeradbiomed.2016.10.507.
[4] D.A. Casciato, M.C. Territo (Eds.), Manual of Clinical Oncology, sixth ed., WolterKluwer/Lippincott Williams& Wilkins, Philadelphia, 2009, pp. 46–99.
[5] M. Bettencourt-Dias, R. Giet, R. Sinka, A. Mazumder, W.G. Look, F. Balloux, P.J. Zafiropoulos, S. Yamaguchi, S. Winter, R.W. Carthew, M. Cooper, D. Jones, et al., Genome-wide survey of protein kinases required for cell cycle progression, Nature 432 (2004) 980–987.
[6] J. Baselga, J. Arribas, Treating cancer's kinase_addiction, Nat. Med. 10 (2004) 786–787.
[7] P. Cohen, Protein kinases—the major drug targets of the twenty-first century? Nat. Rev. Drug Discov. 1 (2002) 309–315, 56.
[8] D.C. Lev, L.S. Kim, V. Melnikova, M. Ruiz, H.N. Ananthaswamy, J.E. Price, Dual blockade of EGFR and ERK1/2 phosphorylation potentiates growth inhibition of breast cancer cells, Br. J. Canc. 91 (2004) 795–802.
[9] M.B. Kastan, J. Bartek, Cell-cycle checkpoints and cancer, Nature 432 (2004) 316–323.
[10] M.A.T.M. Van Vugt, A.K. Gardino, R. Linding, G.J. Ostheimer, H.C. Reinhardt, S.-E. Ong, C.S. Tan, H. Miao, S.M. Keezer, J. Li, T. Pawson, T.A. Lewis, S.A. Carr, S.J. Smerdon, T.R. Brummelkamp, M.B. Yaffe, A mitotic phosphorylation feedback network connects Cdk1, Plk1, 53BP1, and Chk2 to inactivate the g2/m DNA damage checkpoint, PLoS Biol. 8 (2010) 1–8.
[11] R.T. Abraham, PI 3-kinase related kinases: big' players in stress-induced signaling pathways, DNA Repair 3 (2004) 883–887.
[12] F.-F. Hsu, T.-Y. Lin, J.-Y. Chen, S.-Y. Shieh, p53-Mediated transactivation of LIMK2b links act in dynamics to cell cycle checkpoint control, Oncogene 29 (2010) 2864–2876.
[13] S. Matsuoka, M. Huang, S.J. Elledge, Linkage of ATM to cell cycle regulation by the Chk2 protein kinase, Science 282 (1998) 1893–1897.
[14] Y. Shiloh, The ATM-mediated DNA-damage response: taking shape,, Trends Biochem. Sci. 31 (2006) 402–410.
[15] J. Bartek, J. Lukas, Chk1 and Chk2 kinases in checkpoint control and cancer, Canc. Cell 3 (2003) 421–429, 57.
[16] L. Chen, D.M. Gilkes, Y. Pan, W.S. Lane, J. Chen, ATM and Chk2-dependent phosphorylation of MDMX contribute to p53 activation after DNA damage, EMBO J. 24 (2005) 3411–3422.
[17] K. Okamoto, K. Kashima, Y. Pereg, M. Ishida, S. Yamazaki, A. Nota, A. Teunisse, D. Migliorini, I. Kitabayashi, J.-C. Marine, C. Prives, Y. Shiloh, A.G. Jochemsen, Y. Taya, DNA damage-induced phosphorylation of MdmX at serine 367 activates p53 by targeting MdmX for Mdm2-dependent degradation, Mol. Cell Biol. 25 (2005) 9608–9620.
[18] C. Stevens, L. Smith, N.B. La Thangue, Chk2 activates E2F-1 in response to DNA damage, Nat. Cell Biol. 5 (2003) 401–409.
[19] H.A. Rogoff, M.T. Pickering, F.M. Frame, M.E. Debatis, Y. Sanchez, S. Jones, T.F. Kowalik, Apoptosis associated with deregulated E2F activity is dependent on E2F1 and Atm/Nbs1/Chk2, Mol. Cell Biol. 24 (2004) 2968–2977.
[20] Y.-H. Yeh, Y.-F. Huang, T.-Y. Lin, S.-Y. Shieh, The cell cycle checkpoint kinase CHK2 mediates DNA damage induced stabilization of TTK/hMps1, Oncogene 28 (2009) 1366–1378.
[21] Y. Pommier, J.N. Weinstein, M.I. Aladjem, K.W. Kohn, Chk2 molecular interaction map and rationale for Chk2 inhibitors, Clin. Canc. Res. 12 (2006) 2657–2661.
[22] L. Antoni, N. Sodha, I. Collins, M.D. Garrett, Chk2 kinase: cancer susceptibility and cancer therapy - two sides of the same coin? Nat. Rev. Canc. 7 (2007) 925–936.
[23] V. Sharma, C.D. Hupp, J. Tepe, Enhancing the efficacy of chemotherapeutic drugs by small molecule inhibition of nf-kappab and checkpoint kinases, Curr. Med. Chem. 14 (2007) 1061–1074, 58.
[24] J. Ahn, M. Urist, C. Prives, The Chk2 protein kinase, DNA Repair 3 (2004) 1039–1047.
[25] I. Hickson, Y. Zhao, C.J. Richardson, S.J. Green, N.M. Martin, A.I. Orr, P.M. Reaper, S.P. Jackson, N.J. Curtin, G.C. Smith, Identification and characterization of a novel and specific inhibitor of the ataxia-telangiectasia mutated kinase ATM, Canc. Res. 64 (2004) 9152–9159.
[26] A.G. Jobson, J.H. Cardellina II, D. Scudiero, S. Kondapaka, H. Zhang, H. Kim, R. Shoemaker, Y. Pommier, Identification of a bis-guanylhydrazone [4,4-Diacetyldiphenylureabis(guanylhydrazone); NSC 109555] as a novel chemotype for inhibition of Chk2 kinase, Mol. Pharmacol. 72 (2007) 876–884.
[27] J. Chappell, S. Dalton, Altered cell cycle regulation helps stem-like carcinoma cells resist apoptosis, BMC Biol. 8 (2010) 63–65.
[28] M. Castedo, J.L. Perfettini, T. Roumier, K. Yakushijin, D. Horne, R. Medema, G. Kroemer, The cell cycle checkpoint kinase Chk2 is a negative regulator of mitotic catastrophe, Oncogene 23 (2004) 4353–4361.
[29] N.S. Gavande, P.S.V. Vere-Carozza, H.D. Hinshaw, S.I. Jalal, C.R. Sears, K.S. Pawelczak, Turchi, J. J. DNA repair targeted therapy: the past or future of cancer treatment? Pharmacol. Ther. 160 (2016) 65–83.
[30] J. Bartek, J. Falck, J. Lukas, Chk2 kinase — a busy messenger, Nat. Rev. Mol. Cell Biol. 2 (2001) 878–886.
[31] K.L. Arienti, A. Brunmark, F.U. Axe, K. McClure, A. Lee, J. Blevitt, D.K. Neff, L. Huang, S. Crawford, C.R. Pandit, L. Karlsson, J.G. Breitenbucher, Checkpoint kinase inhibitors: SAR and 59 radioprotective properties of a series of 2-arylbenzimidazoles, J. Med. Chem. 48 (2005), 1873–1785.
[32] K.J. McClure, L. Huang, K.L. Arienti, F.U. Axe, A. Brunmark, J. Blevitt, J.G. Breitenbucher, Novel non-benzimidazole chk2 kinase inhibitors, Bioorg. Med. Chem. Lett 16 (2006) 1924–1928.
[33] D.K. Neff, A. Lee-Dutra, J.M. Blevitt, F.U. Axe, M.D. Hack, J.C. Buma, R. Rynberg, A. Brunmark, L. Karlsson, G. Breitenbucher, 2-Aryl benzimidazoles featuring alkyl-linked pendant alcohols and amines as inhibitors of checkpoint kinase Chk2, Bioorg. Med. Chem. Lett 17 (2007) 6467–6471.
[34] J.J. Caldwell, E.J. Welsh, C. Matijssen, V.E. Anderson, L. Antoni, K. Boxall, F. Urban, A. Hayes, F.I. Raynaud, L.J.M. Rigoreau, T. Raynham, G.W. Aherne, L.H. Pearl, A.W. Oliver, M.D. Garrett, I. Collins, Structure-based design of potent and selective 2-(quinazolin-2- yl)phenol inhibitors of checkpoint kinase 2, J. Med. Chem. 54 (2011) 580–590.
[35] S.A. Galal, A.S. Abdelsamie, S.A. Shouman, Y.M. Attia, H.I. Ali, A. Tabll, R. El-Shenawy, Y.S. El Abd, M.M. Ali, A.E. Mahmoud, A.H. Abdel-Halim, A.A. Fyiad, A.S. Girgis, H.I. El-Diwani, Part I: design, synthesis and biological evaluation of novel pyrazole-benzimidazole conjugates as checkpoint kinase 2 (Chk2) inhibitors with studying their activities alone and in combination with genotoxic drugs, Eur. J. Med. Chem. 134 (2017) 392–405.
[36] S.A. Galal, S.H.M. Khairat, H.I. Ali, S.A. Shouman, Y.M. Attia, M.M. Ali, A.E. Mahmoud, A.H. Abdel-Halim, A.A. Fyiad, A. Tabll, R. El-Shenawy, Y.S. El Abd, H.I. El-Diwani, Part II: new candidates of pyrazole-benzimidazole conjugates as checkpoint kinase 2 (Chk2) inhibitors, Eur. J. Med. Chem. 144 (2018) 859–873.
[37] R.S.Z. Saleem, A. Lansdell, J. Tepe, Synthesis and evaluation of debromohymenialdisine derived Chk2 inhibitors, Bioorg. Med. Chem. 20 (2012) 1475–1481 .
[38] H.T. Abdel-Mohsen, F.A.F. Ragab, M.M. Ramla, H.I. El Diwani, Novel benzimidazole-pyrimidine conjugates as potent antitumor agents, Eur. J. Med. Chem. 45 (2010) 2336–2344.
[39] S.A. Galal, A.S. Abdelsamie, H. Tokuda, N. Suzuki, A. Lida, M.M. ElHefnawi, R.A. Ramadan, M.H.E. Atta, H.I. El Diwani, Part I: synthesis, cancer chemopreventive activity and molecular docking study of novel quinoxaline derivatives, Eur. J. Med. Chem. 46 (2011) 327–340.
[40] T. Gregorić, M. Sedić, P. Grbčić, A.T. Paravić, S.K. Pavelić, M. Cetina, R. Vianello, S. Raić- Malić, Novel pyrimidine-2,4-dione–1,2,3-triazole and furo[2,3-*d*]pyrimidine-2-one–1,2,3- triazole hybrids as potential anti-cancer agents: synthesis, computational and X-ray analysis and biological evaluation, Eur. J. Med. Chem. 125 (2017) 1247–1267.
[41] K.M. Foote, K. Blades, A. Cronin, S. Fillery, S.S. Guichard, L. Hassall, I. Hickson, X. Jacq, Discovery of 4-{4-[(3*R*)-3-Methylmorpholin-4-yl]-6-[1-(methylsulfonyl)cyclopropyl] pyrimidin-2-y l}-1*H*-indole (AZ20): a potent and selective inhibitor of ATR protein kinase with monotherapy *in vivo* antitumor activity, J. Med. Chem. 56 (2013) 2125–2138.
[42] F.P. Vendetti, A. Lau, S. Schamus, T.P. Conrads, M.J. O'Connor, C.J. Bakkenist, The orally active and bioavailable ATR kinase inhibitor AZD6738 potentiates the antitumor effects of cisplatin to resolve ATM-deficient non-small cell lung cancer *in vivo*, Oncotarget 6 (2015) 44289–44305.
[43] C. Viegas-Junior, A. Danuello, V. da Silva Bolzani, E.J. Barreiro, C.A.M. Fraga, Molecular hybridization: a useful tool in the design of new drug prototypes, Curr. Med. Chem. 14 (2007) 1829–1852.
[44] L.K. Gediya, V.C. Njar, Promise and challenges in drug discovery and development of hybrid anticancer drugs, Expet Opin. Drug Discov. 4 (2009) 1099–1111.
[45] N.M. Raghavendra, D. Pingili, S. Kadasi, A. Mettu, S.V.U.M. Prasad, Dual or multi-targeting inhibitors: the next generation anticancer agents, Eur. J. Med. Chem. 143 (2018) 1277–1300.
[46] P. Skehan, D. Storeng, R. Scudiero, A. Monks, J. McMahon, D. Vistica, J.T. Warren, H. Bokesch, S. Kenney, M.R. Boyd, New colorimetric cytotoxicity assay for anticancer-drug screening, J. Natl. Cancer Inst. 82 (1990) 1107–1112.
[47] J.W. Janetka, S. Ashwell, Checkpoint kinase inhibitors: a review of the patent literature, Expert Opin. Ther. Pat. 19 (2009) 165–197.
[48] H.U.I. Zhao, H. Piwnica-Worms, ATR-mediated checkpoint pathways regulate phosphorylation and activation of human Chk1, Mol. Cell Biol. 21 (2001) 4129–4139.
[49] X. Liang, Y. Guo, W. Douglas Figg, A.T. Fojo, M.D. Mueller, J.J. Yu, The role of wild-type p53 in cisplatin-induced Chk2 phosphorylation and the inhibition of platinum resistance with a Chk2 inhibitor, Chemother. Res. Pract. 2011 (2010) 1–8.
[50] Z.H. Siddik, Cisplatin: mode of cytotoxic action and molecular basis of resistance, Oncogene 22 (2003) 7265–7279.
[51] L. Carlessi, G. Buscemi, G. Larson, Z. Hong, J.Z. Wu, D. Delia, Biochemical and cellular characterization of VRX0466617, a novel and selective inhibitor for the checkpoint kinase Chk2, Mol. Canc. Therapeut. 6 (2007) 935–944.
[52] A.G. Jobson, G.T. Lountos, P.L. Lorenzi, J. Llamas, J. Connelly, D. Cerna,

J.E. Tropea, A. Onda, G. Zoppoli, S. Kondapaka, Cellular inhibition of checkpoint kinase 2 (Chk2) and potentiation of camptothecins and radiation by the novel Chk2 inhibitor PV1019 [7-nitro-1H-indole-2-carboxylic acid {4-[1-(guanidinohydrazone)-ethyl]-phenyl}-amide], J. Pharmacol. Exp. Therapeut. 331 (2009) 816–826.

[53] H. Towbin, T. Staehelin, J. Gordon, A method has been devised for the electrophoretic transfer of proteins, Proc. Natl. Acad. Sci. USA 76 (1979) 4350–4354.

[54] Molecular Operating Environment (MOE) 2008.10, Chemical Computing Group Inc., Quebec, Canada, 2008.